## FLUX-MORTAR MIXED FINITE ELEMENT METHODS ON NONMATCHING GRIDS\*

WIETSE M. BOON<sup>†</sup>, DENNIS GLÄSER<sup>‡</sup>, RAINER HELMIG<sup>‡</sup>, AND IVAN YOTOV<sup>§</sup>

Abstract. We investigate a mortar technique for mixed finite element approximations of a class of domain decomposition saddle point problems on nonmatching grids in which the variable associated with the essential boundary condition, referred to as flux, is chosen as the coupling variable. It plays the role of a Lagrange multiplier to impose weakly continuity of the variable associated with the natural boundary condition. The flux-mortar variable is incorporated with the use of a discrete extension operator. We present well-posedness and error analysis in an abstract setting under a set of suitable assumptions, followed by a nonoverlapping domain decomposition algorithm that reduces the global problem to a positive definite interface problem. The abstract theory is illustrated for Darcy flow, where the normal flux is the mortar variable used to impose continuity of pressure, and for Stokes flow, where the velocity vector is the mortar variable used to impose continuity of normal stress. In both examples, suitable discrete extension operators are developed and the assumptions from the abstract theory are verified. Numerical studies illustrating the theoretical results are presented for Darcy flow.

**Key words.** flux-mortar method, mixed finite element, domain decomposition, nonmatching grids, a priori error analysis

AMS subject classifications. 65N12, 65N15, 65N55

**DOI.** 10.1137/20M1361407

1. Introduction. The mortar mixed finite element method [4, 5] has proven to be an efficient and flexible nonoverlapping domain decomposition technique for solving a wide range of single-physics or multiphysics problems described by partial differential equations in mixed formulations coupled through interfaces with nonmatching grids. The key attribute of this method is the introduction of a Lagrange multiplier, referred to as the mortar variable, on the interface that enforces continuity of the solution. The method can be implemented as an iterative algorithm that requires only subdomain solves on each iteration.

In this context of porous media flow in a mixed form, the two most natural choices for the mortar variable are the pressure or the normal Darcy flux. In the case of matching grids, domain decomposition methods with these two types of Lagrange multipliers were introduced in [20]. In [4], a mortar mixed finite element method on nonmatching grids with a pressure mortar was developed. A multiscale version of the method, the multiscale mortar mixed finite element method (MMMFEM), was developed in [5]. In this case pressure continuity is enforced by construction and normal flux continuity is enforced in a weak sense. This strategy has been successfully applied

<sup>\*</sup>Received by the editors August 21, 2020; accepted for publication (in revised form) January 6, 2022; published electronically May 31, 2022.

https://doi.org/10.1137/20M1361407

**Funding:** The work of the authors was supported by the Deutsche Forschungsgemeinschaft (DFG, German Research Foundation) funding SFB 1313, project 327154368. The work of the fourth author was supported in part by NSF grants DMS 1818775 and DMS 2111129.

<sup>&</sup>lt;sup>†</sup>Department of Mathematics, KTH Royal Institute of Technology, 114 28 Stockholm, Sweden (wietse@kth.se).

<sup>&</sup>lt;sup>‡</sup>Institute for Modelling Hydraulic and Environmental Systems, University of Stuttgart, 70569 Stuttgart, Germany (dennis.glaeser@iws.uni-stuttgart.de, Rainer.Helmig@iws.uni-stuttgart.de).

<sup>§</sup>Department of Mathematics, University of Pittsburgh, Pittsburgh, PA 15260 USA (yotov@math.pitt.edu).

to more general applications as well, including coupled single-phase and multiphase flows in porous media [31], nonlinear elliptic problems [6], coupled Stokes and Darcy flows [17, 19, 26], and mixed formulations of linear elasticity [23].

In this work, we develop a mortar mixed finite element method for a class of domain decomposition saddle point problems in which the variable associated with the essential boundary condition, referred to as flux, acts as the mortar variable. In this case, the continuity of the trace of the flux is imposed by construction and continuity of the variable associated with the natural boundary condition is imposed weakly. Our specific interest lies in deriving a priori error estimates in the presence of nonmatching grids, i.e., subdomain grids that are chosen entirely independently. To the best of our knowledge, such analysis has not been previously done.

A challenge that arises in this approach is that the interface mortar variable of essential flux type needs to be incorporated into the scheme. We achieve this by introducing an appropriate discrete extension operator in the definition of the discrete flux space. This involves solving subdomain problems with flux boundary conditions. We employ a Lagrange multiplier to remedy both the potential incompatibility of the data as well as the uniqueness of the solution.

Let us highlight the main contributions of this work. First, we develop the method and the theory in a general setting that is applicable to a broad class of saddle point problems. The theory includes well-posedness and a priori error analysis. Our focus is on nonmatching grids and we quantify the role this nonconformity plays in the accuracy of the method. Second, we consider a reduction of the problem to a symmetric, positive definite system that contains only the mortar variable. An iterative scheme is then proposed to solve this reduced system such that the solution possesses a suitable conservation property across the interface at each iteration. Third, we apply the general theory for three important examples, verifying in each case all general assumptions. The leading example is Darcy flow in mixed form, in which the normal flux is the mortar variable that is used to impose weakly continuity of pressure. Two projection operators are proposed that require separate analyses and lead to slightly different error estimates. The second example is Stokes flow, in which the full trace of the velocity vector is the mortar variable, which is used to impose weakly continuity of normal stress. Previously, only normal stress mortar methods for Stokes have been considered, with the mortar variable being used to impose weakly continuity of the velocity [8, 19, 24]. While a velocity Lagrange multiplier has been employed in domain decomposition methods for Stokes with matching grids [27, 29], to the best of our knowledge this is the first Stokes discretization on nonmatching grids with velocity mortar variable. The last example, which is presented as supplementary material (fluxmortar\_suppl.pdf [local/web 299KB]), is coupled Stokes-Darcy problems [13, 17, 19, 26, for which the error analysis of flux-mortar mixed finite element methods has not been studied. This example illustrates the applicability of the general theory to multiphysics problems.

For the sake of clarity of the presentation, we focus on the case of subdomain and mortar grids being on the same scale. However, the flux-mortar mixed finite element method can be formulated as a multiscale method via the use of coarse scale mortar grids, as was done in [5]. In this case, following the approach in [18], the method can be implemented using an interface multiscale pressure basis, which can be computed by solving local subdomain problems with specified mortar flux boundary data.

We note several similarities and relationships between the flux-mortar method and existing schemes. First, as mentioned, our approach is dual to the natural-type mortar technique that is central to the pressure-mortar MMMFEM [4, 5]. Second,

the multiscale hybrid-mixed (MHM) method for second order elliptic problems in primal form [1, 7, 21] similarly introduces flux degrees of freedom on the interfaces between elements to impose weakly continuity of pressure. The analysis of the primal MHM method in an abstract setting can be found in [22]. A MHM method for Stokes flow with a normal stress Lagrange multiplier to impose continuity of the velocity is developed in [2]. In all these instances, the MHM method uses a Lagrange multiplier associated with the natural boundary condition and therefore it does not fit in our fluxmortar framework. Instead, it fits in the natural-type mortar framework. For example, the Stokes method from [2] is closely related to the method developed previously in [19]. Recently, an MHM method for Darcy flow using mixed finite elements for the local solves, which fits in our flux-mortar framework, was investigated in [14]. A main difference with our work is that the method in [14] is defined on a single global grid, allowing for nested refinements of the subdomain grids, whereas the flux-mortar method proposed herein is defined on entirely nonmatching subdomain grids. Our analysis therefore does not exploit the nestedness of the grids and instead relies on the use of discrete projection operators, allowing for more general grid configurations. The MHM method is related to the mixed subgrid upscaling method proposed in [3]. The latter does not involve a Lagrange multiplier, but incorporates global flux continuity via a coarse scale mixed finite element velocity space, which may include additional degrees of freedom internal to the subdomains. In contrast, our method reduces to an interface problem involving only mortar degrees of freedom. Furthermore, the analysis in [3] does not allow for nonmatching grids along the coarse scale interfaces. Finally, we note that the flux-mortar mixed finite element method has been successfully applied in the context of fracture flows [11, 28] and coupled Stokes-Darcy flows [10]. The analysis in [11] exploits that there is tangential flow along the fractures and does not cover the domain decomposition framework considered in this work, while the analysis in [10] focuses on robust preconditioning.

The article is structured as follows. In section 2 we develop the method and theory for a general class of saddle point problems. Section 3 is devoted to the application of the theory to Darcy flow. In section 4 we present and analyze the method for Stokes flow. We verify the theory in the case of Darcy flow with numerical tests in section 5. Conclusions are presented in section 6.

- **2. General setting.** In this section, we introduce the flux-mortar mixed finite element method in a general setting for a wide class of saddle point problems.
- **2.1. Domain decomposition and notation.** Let  $\Omega \subset \mathbb{R}^n$ , n=2,3, be a bounded polygonal domain, decomposed into disjoint polygonal subdomains  $\Omega_i$ ,  $i \in I_{\Omega} = \{1, 2, \dots, n_{\Omega}\}$ . We assume that the measure of  $\Omega$  and of each  $\Omega_i$  is of order one. Let  $\nu_i$  denote the outward unit vector normal to the boundary  $\partial\Omega_i$ . The interface between two subdomains  $\Omega_i$  and  $\Omega_j$  is denoted by  $\Gamma_{ij} := \partial\Omega_i \cap \partial\Omega_j$ . Each interface  $\Gamma_{ij}$  is assumed to be Lipschitz and endowed with a unique, unit normal vector  $\nu$  such that  $\nu := \nu_i = -\nu_j$  on  $\Gamma_{ij}$ , i < j. Let  $\Gamma := \bigcup_{i < j} \Gamma_{ij}$  and  $\Gamma_i := \Gamma \cap \partial\Omega_i$ . We categorize  $\Omega_i$  as an interior subdomain if  $\partial\Omega_i \subseteq \Gamma$ , i.e., if none of its boundaries coincide with the boundary of the domain  $\Omega$ . Let  $I_{int} := \{i \in I_{\Omega} : \partial\Omega_i \subseteq \Gamma\}$ .

We will use the following standard notation. A subscript i on a variable denotes its restriction to  $\Omega_i$ , i.e.,  $w_i := w|_{\Omega_i}$ . For G a domain in  $\mathbb{R}^n$ , n = 2, 3, or a manifold in  $\mathbb{R}^{n-1}$ , the Sobolev spaces on G are denoted by  $W^{k,p}(G)$ . Let  $H^k(G) := W^{k,2}(G)$  and  $L^2(G) := H^0(G)$ . The  $L^2(G)$ -inner product is denoted by  $(\cdot, \cdot)_G$ . Let  $\langle \cdot, \cdot \rangle_{X \times X'}$  denote the duality pairing between X and its dual X', for which we generally omit the subscript. For  $G \subset \mathbb{R}^n$ , let  $H(\operatorname{div}, G) = \{v \in (L^2(G))^n : \{v \in$ 

 $\nabla \cdot \mathbf{v} \in L^2(G)$ . We use the following shorthand notation to denote the norms of these spaces:

$$\|f\|_{k,G} := \|f\|_{H^k(G)}, \quad \|f\|_G := \|f\|_{0,G}, \quad \|\boldsymbol{v}\|_{\mathrm{div},G}^2 := \|\boldsymbol{v}\|_{H(\mathrm{div},G)}^2 = \|\boldsymbol{v}\|_G^2 + \|\nabla \cdot \boldsymbol{v}\|_G^2.$$

We use the binary relation  $a \lesssim b$  to imply that a constant C > 0 exists, independent of the mesh size h, such that  $a \leq Cb$ . The relationship  $\gtrsim$  is defined analogously.

**2.2.** The continuous problem. Given a pair of function spaces  $V \times W$  on  $\Omega$ , we consider the following problem: Find  $(u, p) \in V \times W$  such that

(2.1a) 
$$\sum_{i} a_i(\boldsymbol{u}_i, \boldsymbol{v}_i) - \sum_{i} b_i(\boldsymbol{v}_i, p_i) = \sum_{i} \langle \boldsymbol{g}_i, \boldsymbol{v}_i \rangle \qquad \forall \boldsymbol{v} \in V$$

(2.1a) 
$$\sum_{i} a_{i}(\boldsymbol{u}_{i}, \boldsymbol{v}_{i}) - \sum_{i} b_{i}(\boldsymbol{v}_{i}, p_{i}) = \sum_{i} \langle \boldsymbol{g}_{i}, \boldsymbol{v}_{i} \rangle \qquad \forall \boldsymbol{v} \in V,$$

$$\sum_{i} b_{i}(\boldsymbol{u}_{i}, w_{i}) = \sum_{i} \langle f_{i}, w_{i} \rangle \qquad \forall w \in W.$$

Here  $a_i$  and  $b_i$  are bilinear forms and  $g_i$  and  $f_i$  are functionals. We note that this formulation allows for both essential and natural boundary conditions on  $\partial\Omega$ . Essential boundary conditions are incorporated in the definition of  $V \times W$ . Extensions to other boundary conditions can readily be made.

Let  $V_i$  and  $W_i$  be the respective restrictions of V and W to subdomain  $\Omega_i$  and let  $\|\cdot\|_{V_i}$  and  $\|\cdot\|_{W_i}$  be the associated norms. We then endow  $V\times W$  with the norms

(2.2) 
$$\|\boldsymbol{v}\|_{V} := \sum_{i} \|\boldsymbol{v}_{i}\|_{V_{i}}, \qquad \|\boldsymbol{w}\|_{W} := \sum_{i} \|\boldsymbol{w}_{i}\|_{W_{i}}.$$

The space V is assumed to have sufficient regularity such that a trace operator  $Tr_i$ onto  $\Gamma_i$  for each  $V_i$  is well defined. For homogeneous domain decomposition problems where the same model holds on all subdomains, the space V is characterized by

(2.3) 
$$V = \left\{ \boldsymbol{v} \in \bigoplus_{i} V_i : \operatorname{Tr}_i \boldsymbol{v}_i = \operatorname{Tr}_j \boldsymbol{v}_j \text{ on each } \Gamma_{ij} \right\}.$$

On the other hand, we assume that W is discontinuous across interfaces such that  $W = \bigoplus_i W_i$ . We then introduce the interface space  $\Lambda$  on  $\Gamma$  such that

$$\Lambda|_{\Gamma_i} \subset \operatorname{Tr}_i V_i$$

and endow it with a suitable norm  $\|\cdot\|_{\Lambda}$ . We next list three examples that fit in the general setting. The first two are studied in detail in the forthcoming sections.

Example 2.1 (mixed formulation of Darcy flow, section 3). To model Darcy flow, we let u model the velocity and p the pressure. We then set  $V \times W := H(\operatorname{div}, \Omega) \times I$  $L^2(\Omega)$  and  $\operatorname{Tr}_i$  as the normal trace of the velocity on  $\Gamma_i$ ,  $\operatorname{Tr}_i u_i := \nu \cdot u_i|_{\Gamma_i}$ , ensuring mass conservation. The local bilinear forms are given by  $a_i(\boldsymbol{u}_i, \boldsymbol{v}_i) = (K^{-1}\boldsymbol{u}_i, \boldsymbol{v}_i)_{\Omega_i}$ with K the conductivity tensor and  $b_i(\mathbf{v}_i, p_i) = (\nabla \cdot \mathbf{v}_i, p_i)_{\Omega_i}$ .

Example 2.2 (Stokes flow, section 4). Stokes flow can be modeled in this framework by defining  $V \times W = (H^1(\Omega))^n \times L^2(\Omega)$ ,  $a_i(\boldsymbol{u}, \boldsymbol{v}) = (\tilde{\mu}\varepsilon(\boldsymbol{u}), \varepsilon(\boldsymbol{v}))_{\Omega_i}$  with  $\tilde{\mu}$  the viscosity and  $\varepsilon(\boldsymbol{u})$  the symmetric gradient, and  $b_i(\boldsymbol{v}_i, p_i) = (\nabla \cdot \boldsymbol{v}_i, p_i)_{\Omega_i}$ . In turn,  $\operatorname{Tr}_i \boldsymbol{u}$  is the trace of the entire velocity vector  $\boldsymbol{u}$  on  $\Gamma_i$ ,  $\operatorname{Tr}_i \boldsymbol{u}_i := \boldsymbol{u}_i|_{\Gamma_i}$ .

Example 2.3 (mixed linear elasticity). Let  $u \in V = H(\text{div}, \Omega; \mathbb{R}_{sym}^{n \times n})$  be the symmetric Cauchy stress tensor and let  $p \in W := (L^2(\Omega))^n$  be the displacement field. The operator  $\operatorname{Tr}_i$  is given by the normal trace on  $\Gamma_i$ ,  $\operatorname{Tr}_i u_i := u_i \nu|_{\Gamma_i}$ ; here it enforces conservation of linear momentum. The local systems are then given by  $a_i(u_i, v_i) =$  $(\mathbb{C}^{-1}\boldsymbol{u}_i,\boldsymbol{v}_i)_{\Omega_i}$  in which  $\mathbb{C}^{-1}$  models Hooke's law and  $b_i(\boldsymbol{v}_i,p_i)=(\nabla\cdot\boldsymbol{v}_i,p_i)_{\Omega_i}$ .

**2.3. Discretization.** We next construct the discretization of (2.1). For a subdomain  $\Omega_i$ , let  $\Omega_{h,i}$  be a shape-regular tessellation with typical mesh size h consisting of affine finite elements. The grids  $\Omega_{h,i}$  and  $\Omega_{h,j}$  may be nonmatching along the interface  $\Gamma_{ij}$ . For the interfaces, we introduce a shape-regular affine tessellation of  $\Gamma_{ij}$ , denoted by  $\Gamma_{h,ij}$ , with a typical mesh size  $h_{\Gamma}$ . Let  $\Gamma_h = \bigcup_{i < j} \Gamma_{h,ij}$ 

For each i, let  $V_{h,i} \times W_{h,i} \subset V_i \times W_i$  be a pair of conforming finite element spaces that is stable for the subproblem defined on  $\Omega_i$ . Let  $V_{h,i}^0$  denote the subspace of  $V_{h,i}$  with zero trace on  $\Gamma$  and let  $V_{h,i}^{\Gamma}$  denote the trace space of  $V_{h,i}$  on  $\Gamma_i$ :

(2.4) 
$$V_{h,i}^0 := \{ \boldsymbol{v}_{h,i}^0 \in V_{h,i} : \operatorname{Tr}_i \boldsymbol{v}_{h,i}^0 = 0 \}, \qquad V_h^0 := \bigoplus V_{h,i}^0$$

$$(2.5) V_{h,i}^{\Gamma} := \operatorname{Tr}_{i} V_{h,i}, V_{h}^{\Gamma} := \bigoplus V_{h,i}^{\Gamma}.$$

Let  $\Lambda_h \subset \Lambda$  be the discretization of the interface space. Let  $S_H$  be the null-space

$$(2.6) S_{H,i} := \left\{ w_{h,i} \in W_{h,i} : b_i(\boldsymbol{v}_{h,i}^0, w_{h,i}) = 0, \ \forall \boldsymbol{v}_{h,i}^0 \in V_{h,i}^0 \right\}, S_H := \bigoplus_i S_{H,i}.$$

The subscript H is the characteristic subdomain size.

Next, we define a discrete extension operator  $\mathcal{R}_{h,i}: \Lambda \to V_{h,i}$  in two steps. First, let  $\mathcal{Q}_h: \Lambda \to V_h^{\Gamma}$  be a chosen projection operator and let  $\mathcal{Q}_{h,i}: \Lambda \to V_{h,i}^{\Gamma}$  be its restriction to the trace space of  $V_{h,i}$ . Then, for given  $\lambda \in \Lambda$ , we consider the following problem: Find  $(\mathcal{R}_{h,i}\lambda, p_{h,i}^{\lambda}, r_i) \in V_{h,i} \times W_{h,i} \times S_{H,i}$  such that

(2.7a) 
$$a_i \left( \mathcal{R}_{h,i} \lambda, \mathbf{v}_{h,i}^0 \right) - b_i \left( \mathbf{v}_{h,i}^0, p_{h,i}^{\lambda} \right) = 0 \qquad \forall \mathbf{v}_{h,i}^0 \in V_{h,i}^0,$$

$$(2.7b) b_i(\mathcal{R}_{h,i}\lambda, w_{h,i}) - (r_i, w_{h,i})_{\Omega_i} = 0 \forall w_{h,i} \in W_{h,i},$$

$$(2.7c) (p_{h,i}^{\lambda}, s_i)_{\Omega_i} = 0 \forall s_i \in S_{H,i},$$

(2.7d) 
$$\operatorname{Tr}_{i} \mathcal{R}_{h,i} \lambda = \mathcal{Q}_{h,i} \lambda \qquad \text{on } \Gamma_{i}.$$

Remark 2.1. The space  $S_{H,i}$  serves two purposes. First, it ensures that the problem is solvable, with the Lagrange multiplier  $r_i$  acting as compatible data. Second, due to (2.7c), the auxiliary variable  $p_{h,i}^{\lambda}$  is uniquely defined, i.e., orthogonal to  $S_{H,i}$ .

Let  $\mathcal{R}_h := \bigoplus_i \mathcal{R}_{h,i}$ . In turn, we define the composite spaces  $V_h$  and  $W_h$  as

$$(2.8) V_h := \bigoplus_i \left( V_{h,i}^0 \oplus \mathcal{R}_{h,i} \Lambda_h \right) = V_h^0 \oplus \mathcal{R}_h \Lambda_h, W_h := \bigoplus_i W_{h,i}.$$

We are now ready to set up the flux-mortar mixed finite element method for problem (2.1): Find  $(\boldsymbol{u}_h^0, \lambda_h, p_h) \in V_h^0 \times \Lambda_h \times W_h$  such that

(2.9a) 
$$\sum_{i} a_{i} \left( \boldsymbol{u}_{h,i}^{0} + \mathcal{R}_{h,i} \lambda_{h}, \boldsymbol{v}_{h,i}^{0} \right) - b_{i} \left( \boldsymbol{v}_{h,i}^{0}, p_{h,i} \right) = \sum_{i} \langle \boldsymbol{g}_{i}, \boldsymbol{v}_{h,i}^{0} \rangle \quad \forall \boldsymbol{v}_{h}^{0} \in V_{h}^{0},$$

(2.9b)

$$\sum_{i} a_{i} \left( \boldsymbol{u}_{h,i}^{0} + \mathcal{R}_{h,i} \lambda_{h}, \mathcal{R}_{h,i} \mu_{h} \right) - b_{i} (\mathcal{R}_{h,i} \mu_{h}, p_{h,i}) = \sum_{i} \langle \boldsymbol{g}_{i}, \mathcal{R}_{h,i} \mu_{h} \rangle \quad \forall \mu_{h} \in \Lambda_{h},$$

(2.9c) 
$$\sum_{i} b_{i} \left( \mathbf{u}_{h,i}^{0} + \mathcal{R}_{h,i} \lambda_{h} \right), w_{h,i} = \sum_{i} \langle f_{i}, w_{h,i} \rangle \quad \forall w_{h} \in W_{h}.$$

Remark 2.2. Equation (2.9b) imposes weakly continuity of the variable associated with the natural boundary condition.

To shorten notation, let  $\mathbf{u}_h := \mathbf{u}_h^0 + \mathcal{R}_h \lambda_h$  and  $\mathbf{v}_h := \mathbf{v}_h^0 + \mathcal{R}_h \mu_h$ . Moreover, define  $a(\mathbf{u}, \mathbf{v}) := \sum_i a_i(\mathbf{u}_i, \mathbf{v}_i)$ ,  $b(\mathbf{v}, p) := \sum_i b_i(\mathbf{v}_i, p_i)$ ,  $\langle \mathbf{g}, \mathbf{v} \rangle := \sum_i \langle \mathbf{g}_i, \mathbf{v}_i \rangle$ , and  $\langle f, w \rangle := \sum_i \langle f_i, w_i \rangle$ . Then (2.9) can be equivalently written as follows: Find  $\mathbf{u}_h \in V_h$  and  $p_h \in W_h$  such that

(2.10a) 
$$a(\boldsymbol{u}_h, \boldsymbol{v}_h) - b(\boldsymbol{v}_h, p_h) = \langle \boldsymbol{g}, \boldsymbol{v}_h \rangle \quad \forall \boldsymbol{v}_h \in V_h,$$

(2.10b) 
$$b(\mathbf{u}_h, w_h) = \langle f, w_h \rangle \qquad \forall w_h \in W_h.$$

Note that the flux-mortar mixed finite element method (2.10) is a nonconforming discretization of the weak formulation (2.1), since we generally have  $V_h \not\subset V$ . On the other hand, the definitions do ensure that  $W_h = \bigoplus_i W_{h,i} \subset \bigoplus_i W_i = W$ .

**2.4.** Well-posedness and error analysis. The main results in the a priori analysis of the discrete problem (2.10) are presented in the following three theorems.

Theorem 2.1. Assume the following:

A1. Problem (2.7) has a unique solution and the resulting extension operator  $\mathcal{R}_h$ :  $\Lambda \to V_h$  is continuous, i.e.,

$$\|\mathcal{R}_h \lambda\|_V \lesssim \|\lambda\|_{\Lambda} \qquad \forall \lambda \in \Lambda.$$

A2. The following four inequalities, known as the Brezzi conditions, hold:

$$(2.11a) \quad \forall \boldsymbol{u}_h, \boldsymbol{v}_h \in V_h: \qquad a(\boldsymbol{u}_h, \boldsymbol{v}_h) \lesssim \|\boldsymbol{u}_h\|_V \|\boldsymbol{v}_h\|_V,$$

$$(2.11b) \quad \forall \boldsymbol{v}_h \in V_h \text{ and } w_h \in W_h: \qquad b(\boldsymbol{v}_h, w_h) \lesssim \|\boldsymbol{v}_h\|_V \|w_h\|_W,$$

$$(2.11c) \quad \forall \boldsymbol{v}_h \in V_h \text{ with } b(\boldsymbol{v}_h, w_h) = 0 \ \forall w_h \in W_h: \quad a(\boldsymbol{v}_h, \boldsymbol{v}_h) \gtrsim \|\boldsymbol{v}_h\|_V^2,$$

$$(2.11d) \quad \forall w_h \in W_h, \ \exists \ 0 \neq v_h \in V_h \ such \ that: \qquad b(v_h, w_h) \gtrsim ||v_h||_V ||w_h||_W.$$

Then the discrete problem (2.10) admits a unique solution that satisfies

$$||u_h||_V + ||p_h||_W \lesssim ||g||_{V'} + ||f||_{W'}.$$

*Proof.* Assumption A1 ensures that the space  $V_h$  is well-defined. The well-posedness of (2.10) then follows from (2.11) and standard saddle point theory [9].  $\square$ 

THEOREM 2.2. Assume, in addition to assumptions A1-A2, the following: A3. The following mortar condition holds:

$$\|\mu_h\|_{\Gamma_{ij}} \lesssim \|\mathcal{Q}_{h,i}\mu_h\|_{\Gamma_{ij}} + \|\mathcal{Q}_{h,j}\mu_h\|_{\Gamma_{ij}} \quad \forall \Gamma_{ij}.$$

A4. The following discrete trace inequality holds:

$$\forall i \in I_{\Omega}, \quad \|\operatorname{Tr}_{i} \boldsymbol{v}_{h,i}\|_{\Gamma_{i}} \leq C_{\Gamma,h} \|\boldsymbol{v}_{h,i}\|_{V_{i}} \quad \forall \boldsymbol{v}_{h,i} \in V_{h,i},$$

with  $C_{\Gamma,h}$  possibly depending on h.

Then the mortar solution  $\lambda_h$  of (2.10) is unique.

*Proof.* Since  $u_h = u_h^0 + \mathcal{R}_h \lambda_h$ , it holds that  $\operatorname{Tr}_i u_{h,i} = \mathcal{Q}_{h,i} \lambda_h$ . Then we use A3 and A4 to obtain

$$\|\lambda_h\|_{\Gamma} \lesssim \sum_i \|\mathcal{Q}_{h,i}\lambda_h\|_{\Gamma_i} \leq C_{\Gamma,h} \sum_i \|\boldsymbol{u}_{h,i}\|_{V_i} = C_{\Gamma,h} \|\boldsymbol{u}_h\|_{V}.$$

The result now follows from (2.12).

Remark 2.3. We emphasize that A3 is not necessary to ensure uniqueness of the solution  $(\boldsymbol{u}_h, p_h) \in V_h \times W_h$ , only for the uniqueness of the mortar variable  $\lambda_h$ .

We proceed with the error analysis. Let  $\Pi^V$  and  $\Pi^W$  denote interpolants onto  $V_h$  and  $W_h$ , respectively, with suitable approximation properties.

Theorem 2.3. Assume, in addition to assumptions A1-A2, that the following holds:

A5. The interpolant  $\Pi^V$  is b-compatible in the sense that

$$(2.13) b(\boldsymbol{u} - \Pi^{V} \boldsymbol{u}, w_h) = 0 \quad \forall w_h \in W_h.$$

Then the following a priori error estimate holds:

with  $\mathcal{E}_c$  the consistency error defined as

(2.15) 
$$\mathcal{E}_c := \sup_{0 \neq \boldsymbol{v}_h \in V_h} \frac{a(\boldsymbol{u}, \boldsymbol{v}_h) - b(\boldsymbol{v}_h, p) - \langle \boldsymbol{g}, \boldsymbol{v}_h \rangle}{\|\boldsymbol{v}_h\|_V}.$$

*Proof.* From (2.10) and (2.1b), we obtain the error equations

$$(2.16a) a(\boldsymbol{u} - \boldsymbol{u}_h, \boldsymbol{v}_h) - b(\boldsymbol{v}_h, \Pi^W p - p_h) = a(\boldsymbol{u}, \boldsymbol{v}_h) - b(\boldsymbol{v}_h, \Pi^W p) - \langle \boldsymbol{g}, \boldsymbol{v}_h \rangle,$$

$$(2.16b) b(\Pi^V \boldsymbol{u} - \boldsymbol{u}_h, w_h) = 0,$$

 $\forall (v_h, w_h) \in V_h \times W_h$ , where we used the b-compatibility of  $\Pi^V$  (2.13) from A5 and the fact that  $W_h \subset W$ . It is important to note that we did not use (2.1a), which requires a test function in V. We now set the test functions as

(2.17) 
$$\boldsymbol{v}_h := \Pi^V \boldsymbol{u} - \boldsymbol{u}_h - \delta \boldsymbol{v}_h^p, \quad w_h := \Pi^W p - p_h,$$

where  $\boldsymbol{v}_h^p \in V_h$  is constructed, using the inf-sup condition on b (2.11d) to satisfy

$$(2.18) b(\mathbf{v}_h^p, \Pi^W p - p_h) = \|\Pi^W p - p_h\|_W^2, \|\mathbf{v}_h^p\|_V \lesssim \|\Pi^W p - p_h\|_W,$$

and  $\delta > 0$  is a constant to be chosen later. Now (2.16) leads to

$$a(\Pi^{V}\boldsymbol{u} - \boldsymbol{u}_{h}, \Pi^{V}\boldsymbol{u} - \boldsymbol{u}_{h}) + \delta \|\Pi^{W}p - p_{h}\|_{W}^{2}$$

$$= a(\Pi^{V}\boldsymbol{u} - \boldsymbol{u}, \Pi^{V}\boldsymbol{u} - \boldsymbol{u}_{h}) + a(\boldsymbol{u} - \boldsymbol{u}_{h}, \delta \boldsymbol{v}_{h}^{p})$$

$$- b(\boldsymbol{v}_{h}, \Pi^{W}p - p) + [a(\boldsymbol{u}, \boldsymbol{v}_{h}) - b(\boldsymbol{v}_{h}, p) - \langle \boldsymbol{g}, \boldsymbol{v}_{h} \rangle].$$
(2.19)

For the left-hand side of (2.19), (2.16b) and the coercivity of a (2.11c) in A2 imply

(2.20a) 
$$\|\Pi^{V} \boldsymbol{u} - \boldsymbol{u}_h\|_{V}^{2} \lesssim a(\Pi^{V} \boldsymbol{u} - \boldsymbol{u}_h, \Pi^{V} \boldsymbol{u} - \boldsymbol{u}_h).$$

For first term on the right-hand side of (2.19), we use the continuity of a in A2 and Young's inequality to derive

(2.20b) 
$$a(\Pi^{V}\boldsymbol{u} - \boldsymbol{u}, \Pi^{V}\boldsymbol{u} - \boldsymbol{u}_{h}) \lesssim \frac{1}{2\epsilon_{1}} \|\Pi^{V}\boldsymbol{u} - \boldsymbol{u}\|_{V}^{2} + \frac{\epsilon_{1}}{2} \|\Pi^{V}\boldsymbol{u} - \boldsymbol{u}_{h}\|_{V}^{2}$$

with  $\epsilon_1 > 0$  to be determined later. Similarly, for the second term on the right in (2.19), using  $\epsilon_2 > 0$  and the bound on  $\boldsymbol{v}_h^p$  from (2.18), we obtain

$$(2.20c) a(\mathbf{u} - \mathbf{u}_h, \delta \mathbf{v}_h^p) \lesssim (\|\Pi^V \mathbf{u} - \mathbf{u}\|_V + \|\Pi^V \mathbf{u} - \mathbf{u}_h\|_V) \|\delta \mathbf{v}_h^p\|_V \lesssim \frac{1}{2} \|\Pi^V \mathbf{u} - \mathbf{u}\|_V^2 + \frac{\epsilon_2}{2} \|\Pi^V \mathbf{u} - \mathbf{u}_h\|_V^2 + \left(\frac{1}{2} + \frac{1}{2\epsilon_2}\right) \delta^2 \|\Pi^W p - p_h\|_W^2.$$

For the third right-hand-side term, we use the continuity of b, the properties (2.18), and Young's inequality with  $\epsilon_3 > 0$  to derive

$$b(\boldsymbol{v}_{h}, \Pi^{W} p - p) \lesssim \|\boldsymbol{v}_{h}\|_{V} \|\Pi^{W} p - p\|_{W}$$

$$\lesssim (\|\Pi^{V} \boldsymbol{u} - \boldsymbol{u}_{h}\|_{V} + \delta \|\Pi^{W} p - p_{h}\|_{W}) \|\Pi^{W} p - p\|_{W}$$

$$\lesssim \frac{\epsilon_{3}}{2} \|\Pi^{V} \boldsymbol{u} - \boldsymbol{u}_{h}\|_{V}^{2} + \frac{1}{2} \delta^{2} \|\Pi^{W} p - p_{h}\|_{W}^{2} + \left(\frac{1}{2\epsilon_{3}} + \frac{1}{2}\right) \|\Pi^{W} p - p\|_{W}^{2}.$$

$$(2.20d)$$

Finally, we note that the bracketed terms in (2.19) form the numerator in the consistency error  $\mathcal{E}_c$ . Using the same steps as in (2.20d) with  $\epsilon_4 > 0$  then gives us

$$(2.20e) a(\boldsymbol{u}, \boldsymbol{v}_h) - b(\boldsymbol{v}_h, p) - \langle \boldsymbol{g}, \boldsymbol{v}_h \rangle \leq \|\boldsymbol{v}_h\|_V \mathcal{E}_c$$

$$\lesssim \frac{\epsilon_4}{2} \|\boldsymbol{\Pi}^V \boldsymbol{u} - \boldsymbol{u}_h\|_V^2 + \frac{1}{2} \delta^2 \|\boldsymbol{\Pi}^W p - p_h\|_W^2 + \left(\frac{1}{2\epsilon_4} + \frac{1}{2}\right) \mathcal{E}_c^2.$$

Collecting (2.20) and setting all  $\epsilon_i$  sufficiently small, it follows that

$$\|\Pi^{V} \boldsymbol{u} - \boldsymbol{u}_{h}\|_{V}^{2} + \delta \|\Pi^{W} p - p_{h}\|_{W}^{2}$$

$$\lesssim \|\Pi^{V} \boldsymbol{u} - \boldsymbol{u}\|_{V}^{2} + \|\Pi^{W} p - p\|_{W}^{2} + \delta^{2} \|\Pi^{W} p - p_{h}\|_{W}^{2} + \mathcal{E}_{c}^{2}.$$

Subsequently, we set  $\delta$  sufficiently small to obtain

Combining this with the triangle inequality gives us (2.14).

Remark 2.4. To complete the error estimate, a bound on  $\mathcal{E}_c$  needs to be obtained. We derive such a bound for each example considered in the paper.

2.5. Reduction to an interface problem. We continue by presenting an iterative solution method for the flux-mortar mixed finite element method (2.10) based on the ideas developed in [20] and [36]. In this section, we assume that A3 holds, ensuring that the mortar solution  $\lambda_h$  is unique by Lemma 2.2. The decomposition (2.8) of  $V_h$  into interior and interface degrees of freedom then allows us to reformulate the method as an equivalent problem only in the flux mortar variable  $\lambda_h$ . We recall that the method (2.10) can be written equivalently in the domain decomposition form (2.9). Equation (2.9b) forms the basis for the interface problem. In order to set up this reduced problem, we first solve two subproblems that incorporate the term f and provide the right-hand side for the problem. Next, the reduced problem is set up and solved. Finally, a postprocessing step is necessary to obtain the full solution to the original problem (2.10). For notational brevity, we omit the subscript h on all functions in this section, keeping in mind that all functions are discrete. In the solution process we will utilize a generic extension  $\mathcal{R}_h \mu \in \bigoplus_i V_{h,i}$  such that  $\operatorname{Tr} \mathcal{R}_{h,i} \mu = \mathcal{Q}_{h,i} \mu$ on  $\Gamma_i$ . In practice,  $\tilde{\mathcal{R}}_{h,i}\mu$  can be simply chosen to have all degrees of freedom not associated with  $\Gamma_i$  equal to zero. Recall that  $V_h = \bigoplus_i (V_{h,i}^0 \oplus \mathcal{R}_{h,i} \Lambda)$  with  $\mathcal{R}_{h,i}$  the discrete extension (2.7). Since  $\tilde{\mathcal{R}}_{h,i}\mu = \mathcal{R}_{h,i}\mu + \boldsymbol{v}_{\mu,i}^0$  for some  $\boldsymbol{v}_{\mu,i}^0 \in V_{h,i}^0$ , the spaces  $\bigoplus_i (V_{h,i}^0 \oplus \mathcal{R}_{h,i}\Lambda)$  and  $\bigoplus_i (V_{h,i}^0 \oplus \tilde{\mathcal{R}}_{h,i}\Lambda)$  are the same.

We will also utilize the orthogonal decomposition  $\Lambda_h = \Lambda_h^0 \oplus \overline{\Lambda}_h$ , where

(2.22) 
$$\Lambda_h^0 := \{ \mu \in \Lambda_h : b(\tilde{\mathcal{R}}_h \mu, s) = 0 \ \forall s \in S_H \}.$$

To continue, we make the following assumption.

A6. The following inf-sup condition holds for the spaces  $\Lambda_h \times S_H$ :

$$\forall s_H \in S_H, \ \exists 0 \neq \mu_h \in \Lambda_h \ such \ that: \quad b(\mathcal{R}_h \mu_h, s_H) \gtrsim \|\mu_h\|_{\Lambda} \|s_H\|_{W}.$$

Let 
$$B: \Lambda_h \to S'_H$$
 be defined as  $\forall \mu \in \Lambda_h, \langle B\mu, s \rangle := b(\tilde{\mathcal{R}}_h \mu, s) \ \forall s \in S_H$ .

LEMMA 2.4. If A6 holds, then B is an isomorphism from  $\overline{\Lambda}_h$  to  $S'_H$  and  $B^T$  is an isomorphism from  $S_H$  to  $\overline{\Lambda}'_h$ .

*Proof.* The two statements are equivalent and we prove the latter. We note that  $\ker B = \Lambda_h^0$ . Using [33, Proposition 7.4.1], the inf-sup condition A6 implies that  $B^T$  is an isomorphism from  $S_H$  to the polar set of  $\ker B$ ,  $\{g \in \Lambda_h' : \langle g, \mu \rangle = 0 \ \forall \ \mu \in \ker B\}$ , which is exactly  $\overline{\Lambda}_h'$ .

With these prerequisites in place, we describe the iterative solution method in four steps.

The first step aims to capture the influence of f in (2.9c) with respect to the space  $S_H$  (cf. (2.6)). We solve the following global coarse problem: Find  $\overline{\lambda}_f \in \overline{\Lambda}_h$  such that

$$(2.23) b(\tilde{\mathcal{R}}_h \overline{\lambda}_f, s) = \langle f, s \rangle \quad \forall s \in S_H.$$

This problem has the form  $B\overline{\lambda}_f = f$  with  $f \in S'_H$ . Thus, it has a unique solution, since  $B : \overline{\Lambda}_h \to S'_H$  is an isomorphism.

Second, we use  $\lambda_f$  to solve independent, local subproblems to satisfy (2.9a) and capture the remaining influence of f in (2.9c): Find  $(\boldsymbol{u}_f^0, p_f^0, r_f) \in V_h^0 \times W_h \times S_H$  such that

$$(2.24a) a(\mathbf{u}_f^0, \mathbf{v}^0) - b(\mathbf{v}^0, p_f^0) = -a(\tilde{\mathcal{R}}_h \overline{\lambda}_f, \mathbf{v}^0) + \langle g, \mathbf{v}^0 \rangle \forall \mathbf{v}^0 \in V_h^0,$$

(2.24b) 
$$b\left(\mathbf{u}_{f}^{0},w\right)-(r_{f},w)_{\Omega}=-b(\tilde{\mathcal{R}}_{h}\overline{\lambda}_{f},w)+\langle f,w\rangle \qquad \forall w\in W_{h}$$

$$(2.24c) (p_f^0, s)_{\Omega} = 0 \forall s \in S_H.$$

Here, we enforce  $p_f^0 \perp S_H$  with the use of a Lagrange multiplier  $r_f$ . The well-posedness of (2.24) follows from the solvability of the discrete extension problem (2.7) in A1. We further note that setting  $w = r_f \in S_H$  and using (2.23) implies that  $r_f = 0$ . Therefore, the variable  $\boldsymbol{u}_f := \boldsymbol{u}_f^0 + \tilde{\mathcal{R}}_h \overline{\lambda}_f$  satisfies (2.9c). In addition,  $\boldsymbol{u}_f$  and  $p_f^0$  satisfy (2.9a).

It remains to satisfy the continuity equation (2.9b), which is done in two steps. To satisfy it in  $\Lambda_h^0$ , we solve the interface problem: Find  $\lambda^0 \in \Lambda_h^0$  such that

$$(2.25) \quad a(\mathcal{R}_h \lambda^0, \tilde{\mathcal{R}}_h \mu^0) - b(\tilde{\mathcal{R}}_h \mu^0, p^{\lambda^0}) = -a(\boldsymbol{u}_f, \tilde{\mathcal{R}}_h \mu^0) + b(\tilde{\mathcal{R}}_h \mu^0, p_f^0) \quad \forall \mu^0 \in \Lambda_h^0,$$

in which the pair  $(\mathcal{R}_h \lambda^0, p^{\lambda^0})$  solves the discrete extension problem (2.7). The solvability of (2.25) is established in Lemma 2.5 below.

After solving the interface problem, we require a fourth, final step to guarantee that (2.9b) holds in  $\overline{\Lambda}_h$ , which is also used to obtain the correct variable p. Thus, we construct  $\overline{p}_{\lambda} \in S_H$  such that

$$(2.26) b(\tilde{\mathcal{R}}_h \overline{\mu}, \overline{p}_{\lambda}) = a(\boldsymbol{u}_f + \mathcal{R}_h \lambda^0, \tilde{\mathcal{R}}_h \overline{\mu}) - b(\tilde{\mathcal{R}}_h \overline{\mu}, p^{\lambda^0} + p_f^0) \forall \overline{\mu} \in \overline{\Lambda}_h,$$

which results in a coarse grid problem of the form  $B^T \overline{p}_{\lambda} = \overline{g}$  in  $\overline{\Lambda}'_h$ . Since  $B^T : S_H \to \overline{\Lambda}'_h$  is an isomorphism, the problem has a unique solution.

We now have all the necessary ingredients to construct

(2.27) 
$$\mathbf{u} := \mathbf{u}_f + \mathcal{R}_h \lambda^0 = \mathbf{u}_f^0 + \mathcal{R}_h \lambda^0 + \tilde{\mathcal{R}}_h \overline{\lambda}_f, \quad p := p_f^0 + p^{\lambda^0} + \overline{p}_{\lambda}.$$

It is elementary to check that  $(u, p) \in V_h \times W_h$  indeed solves (2.10). The corresponding mortar variable is  $\lambda = \lambda^0 + \overline{\lambda}_f$ . We next show the solvability of (2.25).

LEMMA 2.5. If A3 holds, then the bilinear form of the reduced problem (2.25), given by

(2.28) 
$$a_{\Gamma}(\lambda,\mu) := a(\mathcal{R}_h\lambda,\tilde{\mathcal{R}}_h\mu) - b(\tilde{\mathcal{R}}_h\mu,p^{\lambda}),$$

is symmetric and positive definite in  $\Lambda_h^0 \times \Lambda_h^0$ .

*Proof.* Using that  $\tilde{\mathcal{R}}_h \mu = \mathcal{R}_h \mu + \boldsymbol{v}_{\mu}^0$  for some  $\boldsymbol{v}_{\mu}^0 \in V_h^0$ , we have

$$a_{\Gamma}(\lambda,\mu) = a(\mathcal{R}_h\lambda, \mathcal{R}_h\mu) - b(\mathcal{R}_h\mu, p^{\lambda}) + a\left(\mathcal{R}_h\lambda, \mathbf{v}_{\mu}^{0}\right) - b\left(\mathbf{v}_{\mu}^{0}, p^{\lambda}\right)$$
$$= a(\mathcal{R}_h\lambda, \mathcal{R}_h\mu) - b\left(\mathcal{R}_h\mu, p^{\lambda}\right) = a(\mathcal{R}_h\lambda, \mathcal{R}_h\mu).$$

Here we used (2.7a) in the second equality. For the last equality we used that, on the one hand,  $b_i(\mathcal{R}_{h,i}\mu,s_{H,i})=b_i(\tilde{\mathcal{R}}_{h,i}\mu-\boldsymbol{v}_{\mu,i}^0,s_{H,i})=0 \ \forall s_{H,i} \in S_{H,i}$  due to the fact that  $\mu \in \Lambda_h^0$  and (2.6). On the other hand, (2.7b) gives us that  $b_i(\mathcal{R}_{h,i}\mu,w_{h,i})=(r_i,w_{h,i})_{\Omega_i}=0 \ \forall w_{h,i} \perp S_{H,i}$ , thus  $b(\mathcal{R}_h\mu,p^\lambda)=0$ . We conclude that  $a_{\Gamma}(\lambda,\mu)$  is symmetric and positive semidefinite in  $\Lambda_h^0 \times \Lambda_h^0$ . Moreover, if  $\mathcal{R}_h\lambda=0$ , then its trace  $\mathcal{Q}_h\lambda$  is zero as well and so  $\lambda=0$  due to A3. Hence  $a_{\Gamma}$  is positive definite.

The main implication of Lemma 2.5 is that the interface problem (2.25) can be solved using iterative methods such as the conjugate gradient method. An important observation is that the second equation (2.10b) is satisfied by construction, even if the iterative solver is terminated before convergence. Specifically, the component  $u_f$  is computed a priori and the update defined by  $\lambda^0$  only improves the accuracy of the solution with respect to (2.10a). This property is particularly attractive if (2.10b) describes a physically important conservation equation and (2.10a) models a constitutive relationship between u and p.

Remark 2.5. The implementation of problems (2.23) and (2.26) requires solving a system with the same coarse matrix. The same system also occurs in the computation of the projection onto  $\Lambda_h^0$  required in (2.25). We refer the reader to [37] for an algebraic formulation for solving a global saddle problem with singular subdomain problems of a type similar to (2.10), which is based on the FETI method [36]. We note that the incorporation of the coarse problem results in convergence of the interface iterative solver that is independent of the subdomain size.

**3.** Darcy flow. We exemplify the flux-mortar mixed finite element method using an accessible model problem given by the mixed formulation of the Poisson problem:

(3.1) 
$$\mathbf{u} = -K\nabla p, \quad \nabla \cdot \mathbf{u} = f \text{ in } \Omega, \quad p = 0 \text{ on } \partial\Omega.$$

We will use the terminology common to porous media flow modeling. Hence, we refer to  $\boldsymbol{u}$  as the Darcy velocity, p is the pressure, K is a uniformly bounded symmetric positive definite conductivity tensor, and  $f \in L^2(\Omega)$  is a source function. We assume that there exist  $0 < k_{min} \le k_{max} < \infty$  such that  $\forall \boldsymbol{x} \in \Omega$ ,

(3.2) 
$$k_{min}\xi^T\xi \le \xi^T K(x)\xi \le k_{max}\xi^T\xi \quad \forall \xi \in \mathbb{R}^n.$$

The variational formulation of (3.1) is, Find  $(\boldsymbol{u},p) \in V \times W := H(\operatorname{div},\Omega) \times L^2(\Omega)$  such that

$$(3.3a) (K^{-1}\boldsymbol{u},\boldsymbol{v})_{\Omega} - (\nabla \cdot \boldsymbol{v},p)_{\Omega} = 0 \forall \boldsymbol{v} \in V,$$

(3.3b) 
$$(\nabla \cdot \boldsymbol{u}, w)_{\Omega} = (f, w)_{\Omega} \qquad \forall w \in W.$$

It is well known that (3.3) has a unique solution [9]. Note that (3.3a) implies that  $p \in H_0^1(\Omega)$ , hence the solution to (3.3) satisfies (3.1).

For given  $\Omega_i$ , the local velocity and pressure function spaces are defined as  $V_i := H(\text{div}, \Omega_i)$  and  $W_i := L^2(\Omega_i)$ , respectively. Problem (3.3) attains the form (2.1) with

$$(3.4)$$

$$a_i(\boldsymbol{u}_i, \boldsymbol{v}_i) = (K^{-1}\boldsymbol{u}_i, \boldsymbol{v}_i)_{\Omega_i}, \quad b_i(\boldsymbol{v}_i, p_i) = (\nabla \cdot \boldsymbol{v}_i, p_i)_{\Omega_i}, \quad \boldsymbol{g} = 0, \quad \langle f, w \rangle = (f, w)_{\Omega_i}.$$

The global space V possesses continuity of the normal trace on  $\Gamma$ . Thus, following (2.3), we set

$$\operatorname{Tr}_i \boldsymbol{u}_i := (\boldsymbol{\nu} \cdot \boldsymbol{u}_i)|_{\Gamma_i}, \quad \Lambda := L^2(\Gamma).$$

We note that  $\Lambda$  has more regularity than the normal trace of V, which is a distributional space with a norm related to  $H^{-1/2}(\Gamma)$ . This choice allows us to employ the  $L^2$ -projection in the definition of the projection operator  $\mathcal{Q}_{h,i}: \Lambda \to V_{h,i}^{\Gamma}$ . The  $L^2$ -projection is easier to implement and the  $L^2(\Gamma)$ -norm for the mortar variable is easier to compute than their distributional counterparts. For  $\lambda \in \Lambda$ , we use a subscript to indicate its relative orientation with respect to the adjacent subdomains:

$$\lambda_i := \lambda, \ \lambda_j := -\lambda \ \text{on } \Gamma_{ij}, \ i < j.$$

In particular,  $\lambda_i$  models  $\boldsymbol{\nu}_i \cdot \boldsymbol{u}$  and  $\lambda_j$  models  $\boldsymbol{\nu}_j \cdot \boldsymbol{u}$  on  $\Gamma_{ij}$ .

Next, we associate appropriate norms to the function spaces. The spaces W and  $\Lambda$  are equipped with the standard  $L^2(\Omega)$  and  $L^2(\Gamma)$  norms, respectively, and the space V is equipped with a broken H(div) norm:

$$\| m{v} \|_V := \sum_i \| m{v}_i \|_{\mathrm{div},\Omega_i}, \qquad \quad \| m{w} \|_W := \| m{w} \|_{\Omega}, \qquad \quad \| m{\mu} \|_{\Lambda} := \| m{\mu} \|_{\Gamma}.$$

**3.1. Discretization.** In this section we describe the flux-mortar mixed finite element method for (3.3). Since the local finite element spaces are required to be stable for the subproblems defined on each  $\Omega_i$ , we choose  $V_{h,i} \times W_{h,i}$  such that

$$(3.5a) \quad \nabla \cdot V_{h,i} = W_{h,i},$$

$$(3.5b) \quad \forall w_{h,i} \in W_{h,i}, \ \exists \ 0 \neq v_{h,i} \in V_{h,i} : (\nabla \cdot v_{h,i}, w_{h,i})_{\Omega_i} \gtrsim \|v_{h,i}\|_{\operatorname{div},\Omega_i} \|w_{h,i}\|_{\Omega_i}.$$

Stable Darcy pairs (see, e.g., [9, Chapter 2]) include the Raviart-Thomas and the Brezzi-Douglas-Marini elements. Let the discrete interface space  $\Lambda_{h,ij} \subset L^2(\Gamma_{ij})$  contain continuous or discontinuous piecewise polynomials on  $\Gamma_{h,ij}$ .

For the projection operator  $\mathcal{Q}_h: \Lambda \to V_h^{\Gamma}$  (see (2.5)), we consider two options, which we distinguish using a superscript  $\flat$  or  $\sharp$ . The first option ( $\flat$ ) is defined using the  $L^2$ -projection to each trace space  $V_{h,i}^{\Gamma}$  such that the extension satisfies

(3.6a) 
$$(\lambda_i - \boldsymbol{\nu}_i \cdot \mathcal{R}_{h,i}^{\flat} \lambda, \xi_{h,i})_{\Gamma_i} = 0 \qquad \forall \xi_{h,i} \in V_{h,i}^{\Gamma}.$$

The second option (#) results in an extension such that its normal trace has zero jump with respect to the mortar space:

(3.6b) 
$$\sum_{i} (\boldsymbol{\nu}_{i} \cdot \mathcal{R}_{h,i}^{\sharp} \lambda, \mu_{h})_{\Gamma_{i}} = 0 \qquad \forall \mu_{h} \in \Lambda_{h}.$$

The construction of these projection operators is described in detail in sections 3.1.2 and 3.1.1. The extension operator  $\mathcal{R}_h$  is then defined according to (2.7), which we describe in detail in section 3.1.3.

After choosing  $\mathcal{R}_h$ , the composite spaces  $V_h$  and  $W_h$  are given by (2.8). The two variants of  $V_h$  that arise due to the choice of  $\mathcal{Q}_{h,i}$  are denoted by  $V_h^{\sharp}$  and  $V_h^{\flat}$ . We will present the results that concern both variants by omitting the superscript.

Following (2.9) and (2.10), the flux-mortar mixed finite element method is as follows: Find  $\mathbf{u}_h \in V_h$  and  $p_h \in W_h$  such that

(3.7a) 
$$(K^{-1}\boldsymbol{u}_h, \boldsymbol{v}_h)_{\Omega} - \sum_{i} (\nabla \cdot \boldsymbol{v}_h, p_h)_{\Omega_i} = 0 \qquad \forall \boldsymbol{v}_h \in V_h$$

(3.7a) 
$$(K^{-1}\boldsymbol{u}_h, \boldsymbol{v}_h)_{\Omega} - \sum_{i} (\nabla \cdot \boldsymbol{v}_h, p_h)_{\Omega_i} = 0 \qquad \forall \boldsymbol{v}_h \in V_h,$$

$$\sum_{i} (\nabla \cdot \boldsymbol{u}_h, w_h)_{\Omega_i} = (f, w_h)_{\Omega} \qquad \forall w_h \in W_h.$$

Equation (2.9b), which here is  $\sum_{i} \left( (K^{-1} \boldsymbol{u}_{h,i}, \mathcal{R}_{h,i} \mu_h)_{\Omega_i} - (\nabla \cdot \mathcal{R}_{h,i} \mu_h, p_{h,i})_{\Omega_i} \right) = 0$  $\forall \mu_h \in \Lambda_h$ , imposes weakly continuity of pressure.

We next focus on the two types of extension operators  $\mathcal{R}_h^{\sharp}$  and  $\mathcal{R}_h^{\flat}$ .

**3.1.1. Projection to the trace spaces.** The projection operator  $\mathcal{Q}_h^{\flat}: \Lambda \to V_h$ that leads to (3.6a) is the  $L^2(\Gamma_i)$ -orthogonal projection onto  $V_{h,i}^{\Gamma}$ , which is computed for each i by solving the problem, Given  $\lambda \in \Lambda$ , find  $\mathcal{Q}_{h,i}^{\flat} \lambda \in V_{h,i}^{\Gamma}$  such that

(3.8) 
$$(\lambda_i - \mathcal{Q}_{h,i}^{\flat} \lambda, \xi_{h,i})_{\Gamma_i} = 0 \quad \forall \, \xi_{h,i} \in V_{h,i}^{\Gamma}.$$

We will make use of the property

(3.9) 
$$(\lambda_i - \mathcal{Q}_{h,i}^{\flat} \lambda, 1)_{\Gamma_{ij}} = 0 \quad \forall \Gamma_{ij},$$

which follows from the fact that the indicator function of  $\Gamma_{ij}$  is in the space  $V_{h,i}^{\Gamma}$ .

By solving (2.7), the extension  $\mathcal{R}_{h,i}^{\flat}$  is then created such that  $\nu_i \cdot \mathcal{R}_{h,i}^{\flat} \lambda = \mathcal{Q}_{h,i}^{\flat} \lambda$ on  $\Gamma_i$  (see section 3.1.3). We refer to the resulting function space as  $V_h^{\flat} := V_h^0 \oplus \mathcal{R}_h^{\flat} \Lambda_h$ .

**3.1.2.** Projection to the space of weakly continuous functions. An alternative choice of the projection operator ( $\sharp$ ) aims to satisfy (3.6b). In its construction, we use the concept of weakly continuous functions, as introduced in [4] in the pressuremortar method. In particular, let the space of weakly continuous fluxes  $V_{h,c}$  and the associated trace space  $V_{h,c}^{\Gamma}$  be given by

$$\begin{split} V_{h,c} &:= \left\{ \boldsymbol{v}_h \in \bigoplus_i V_{h,i} : \ \sum_i (\boldsymbol{\nu}_i \cdot \boldsymbol{v}_{h,i}, \mu_h)_{\Gamma_i} = 0 \ \forall \mu_h \in \Lambda_h \right\}, \\ V_{h,c}^{\Gamma} &:= \left\{ \xi_h \in V_h^{\Gamma} : \ \sum_i (\xi_{h,i}, \mu_h)_{\Gamma_i} = 0 \ \forall \mu_h \in \Lambda_h \right\}. \end{split}$$

We construct the projection  $\mathcal{Q}_h^{\sharp}:\Lambda\to V_h^{\Gamma}$  by solving the following auxiliary problem, obtained from [4]: Given  $\lambda \in \Lambda$ , find  $Q_h^{\sharp} \lambda \in V_h^{\Gamma}$  and  $\chi_h \in \Lambda_h$  such that

(3.10a) 
$$\sum_{i} (\lambda_i - \mathcal{Q}_{h,i}^{\sharp} \lambda - \chi_h, \xi_{h,i})_{\Gamma_i} = 0 \qquad \forall \xi_h \in V_h^{\Gamma},$$

(3.10b) 
$$\sum_{i} (\mathcal{Q}_{h,i}^{\sharp} \lambda, \mu_h)_{\Gamma_i} = 0 \qquad \forall \mu_h \in \Lambda_h.$$

LEMMA 3.1. If A3 holds for  $Q_h^b$ , then problem (3.10) admits a unique solution.

*Proof.* Since (3.10) corresponds to a square system of equations, it suffices to show uniqueness. Hence, we set  $\lambda = 0$  and choose  $\xi_{h,i} = \mathcal{Q}_{h,i}^{\sharp} \lambda$  and  $\mu_h = \chi_h$ . It follows after summation of the two equations that  $\mathcal{Q}_{h,i}^{\sharp} \lambda = 0$ . The first equation then implies that  $\mathcal{Q}_{h}^{\flat} \chi_{h} = 0$  and, using A3 for  $\mathcal{Q}_{h}^{\flat}$ , we have  $\chi_{h} = 0$ .

Lemma 3.2. The solution  $\mathcal{Q}_h^{\sharp}\lambda$  of (3.10) is the  $L^2$ -projection of  $\lambda$  onto  $V_{h,c}^{\Gamma}$ . Moreover, it satisfies

$$(3.11) (\lambda_i - \mathcal{Q}_{h,i}^{\sharp} \lambda, 1)_{\Gamma_{ij}} = 0 \quad \forall \Gamma_{ij}.$$

*Proof.* First, we note that  $\mathcal{Q}_h^{\sharp} \lambda \in V_{h,c}^{\Gamma}$  due to (3.10b). By choosing  $\xi_h$  in (3.10a) from  $V_{h,c}^{\Gamma} \subset V_h^{\Gamma}$ , we obtain

$$\sum_{i} (\lambda_i - \mathcal{Q}_{h,i}^{\sharp} \lambda, \xi_{h,i})_{\Gamma_i} = 0 \qquad \forall \xi_h \in V_{h,c}^{\Gamma}.$$

Hence,  $Q_h^{\sharp}\lambda$  is the  $L^2$ -projection of  $\lambda$  onto  $V_{h,c}^{\Gamma}$ . For the second result, we consider a given  $\Gamma_{ij}$  and note that  $1 \in V_{h,i}^{\Gamma} \cap V_{h,j}^{\Gamma}$ . Taking  $\xi_{h,i} = \xi_{h,j} = 1$  on  $\Gamma_{ij}$  in (3.10a) and using that  $1 \in \Lambda_{h,ij}$  and  $Q_h^{\sharp}\lambda \in V_{h,c}^{\Gamma}$ , we derive

$$2(\chi_h, 1)_{\Gamma_{ij}} = (\lambda_i - \mathcal{Q}_{h,i}^{\sharp} \lambda, 1)_{\Gamma_{ij}} + (\lambda_j - \mathcal{Q}_{h,j}^{\sharp} \lambda, 1)_{\Gamma_{ij}}$$
$$= (\lambda_i + \lambda_j, 1)_{\Gamma_{ij}} - (\mathcal{Q}_{h,i}^{\sharp} \lambda + \mathcal{Q}_{h,j}^{\sharp} \lambda, 1)_{\Gamma_{ij}} = 0.$$

Thus, taking  $\xi_{h,i} = 1$  and  $\xi_{h,j} = 0$  on  $\Gamma_{ij}$  in (3.10a) gives  $(\lambda_i - \mathcal{Q}_{h,i}^{\sharp}\lambda, 1)_{\Gamma_{ij}} = 0$ .

The second step is to define the bounded extension  $\mathcal{R}_{h,i}^{\sharp}$  to the discrete space  $V_{h,i}$  using (2.7) such that  $\nu_i \cdot \mathcal{R}_{h,i}^{\sharp} \lambda = \mathcal{Q}_{h,i}^{\sharp} \lambda$  on  $\Gamma_i$  (see section 3.1.3). Let  $V_h^{\sharp} := V_h^0 \oplus \mathcal{R}_h^{\sharp} \Lambda_h$  be the resulting discrete function space.

Remark 3.1. Lemma 3.1 shows that A3 for  $\mathcal{Q}_h^{\flat}$  is needed for  $\mathcal{Q}_h^{\sharp}$  to be well-defined. From here on, we will therefore assume that this condition is satisfied whenever  $\mathcal{Q}_h^{\sharp}$  or  $\mathcal{R}_h^{\sharp}$  is used.

Remark 3.2. Assumption A3 is the conventional mortar assumption (see, e.g., [4, 5]) implying that the mortar variable is controlled on each interface by its  $L^2$ -projection onto one of the two neighboring subdomains. The assumption is easy to satisfy in practice by choosing a sufficiently coarse mortar grid  $\Gamma_h$  and it has been shown to hold for some very general mesh configurations [30], including cases with a polynomial degree in  $\Lambda_h$  higher than the polynomial degree in  $V_h^{\Gamma}$ . A related coarseness assumption is considered in [7]. Furthermore, A3 holds trivially in the special case  $\Lambda_{h,i} \subseteq V_{h,i}^{\Gamma}$ , which is considered in [14].

Remark 3.3. Due to Lemma 3.2, we note that  $V_h^{\sharp} \subseteq V_{h,c}$ . However, the converse inclusion does not hold in general since the projection  $\mathcal{Q}_h^{\sharp}$  is not necessarily surjective on  $V_{h,c}^{\Gamma}$  when acting on  $\Lambda_h$ . Therefore, the problem we set up in  $V_h^{\sharp}$  is closely related, but not equivalent, to the one introduced in [4, section 3]. To be specific, we have used  $\mathcal{R}_h^{\sharp}$  to generate a strict subspace of  $V_{h,c}$  whereas the problem in [4] is posed on  $V_{h,c}$ .

Remark 3.4. The spaces  $V_h^{\sharp}$  and  $V_h^{\flat}$  are different in general, with none contained in the other. This can be seen by the fact that both spaces have the same, finite dimensionality but the extension  $\mathcal{R}_h^{\flat}$  does not satisfy (3.6b) in general.

**3.1.3.** The extension operator. We next present the extension operator  $\mathcal{R}_{h,i}$ into  $V_{h,i}$ . It is denoted by  $\mathcal{R}_{h,i}^{\sharp}$  or  $\mathcal{R}_{h,i}^{\flat}$  depending on the associated projection operator  $\mathcal{Q}_h^{\sharp}$  or  $\mathcal{Q}_h^{\flat}$ . We refer to results concerning both extension operators by omitting the superscript.

Following (2.7), the discrete extension operator on each subdomain  $\Omega_i$  will be defined using a subdomain problem with Neumann data on  $\Gamma_i$ . For interior subdomains,  $i \in I_{int}$ , this results in Neumann boundary conditions on the entire boundary  $\partial\Omega_i$ . To deal with possibly singular subdomain problems, we define the space  $S_H$  as in (2.6), which in this case is given by

$$(3.12) S_{H,i} := \begin{cases} \mathbb{R}, & i \in I_{int}, \\ 0, & i \notin I_{int}, \end{cases} S_H := \bigoplus_i S_{H,i}.$$

We now set up problem (2.7) to define the extension  $\mathcal{R}_{h,i}\lambda$  for given  $\lambda \in \Lambda$ : Find  $(\mathcal{R}_{h,i}\lambda, p_{h,i}^{\lambda}, r_i) \in V_{h,i} \times W_{h,i} \times S_{H,i}$  such that

(3.13b) 
$$(\nabla \cdot \mathcal{R}_{h,i}\lambda, w_{h,i})_{\Omega_i} - (r_i, w_{h,i})_{\Omega_i} = 0 \qquad \forall w_{h,i} \in W_{h,i},$$

$$(3.13b) \qquad (\nabla \cdot \mathcal{R}_{h,i}\lambda, w_{h,i})_{\Omega_i} \qquad (\nabla \cdot \mathcal{R}_{h,i}\lambda, w_{h,i})_{\Omega_i} = 0 \qquad \forall w_{h,i} \in \mathcal{H}_h, \\ (3.13c) \qquad (p_{h,i}^{\lambda}, s_i)_{\Omega_i} = 0 \qquad \forall s_i \in S_{H,i}, \\ (3.13d) \qquad \qquad \boldsymbol{\nu}_i \cdot \mathcal{R}_{h,i}\lambda = \mathcal{Q}_{h,i}\lambda \qquad \text{on } \Gamma_i.$$
We note that (3.13d) is an essential boundary condition and that, for substitution of the condition of the condition

(3.13d) 
$$\nu_i \cdot \mathcal{R}_{h,i} \lambda = \mathcal{Q}_{h,i} \lambda \qquad \text{on } \Gamma_i$$

We note that (3.13d) is an essential boundary condition and that, for subdomains adjacent to  $\partial\Omega$ , the boundary condition  $p_i^{\lambda}=0$  on  $\partial\Omega_i\setminus\Gamma_i$  is natural and has been incorporated in (3.13a). We emphasize the use of  $Q_{h,i}\lambda = Q_{h,i}^{\flat}\lambda$  from (3.8) in (3.13d) leads to  $\mathcal{R}_{h,i} = \mathcal{R}_{h,i}^{\flat}$ , while  $\mathcal{Q}_{h,i}\lambda = \mathcal{Q}_{h,i}^{\sharp}\lambda$  from (3.10) results in  $\mathcal{R}_{h,i} = \mathcal{R}_{h,i}^{\sharp}$ .

Remark 3.5. Problem (3.13) is similar to the downscaling stage in [14]. The main difference is that here, the boundary data is first projected using  $Q_h$  to account for the fact that  $\Lambda_{h,i} \not\subseteq V_{h,i}^{\Gamma}$ .

Lemma 3.3 (A1). Problem (3.13) admits a unique solution with

(3.14) 
$$\nabla \cdot \mathcal{R}_{h,i} \lambda = \overline{\lambda}_i \qquad and \qquad \|\mathcal{R}_{h,i} \lambda\|_{\operatorname{div},\Omega_i} \lesssim \|\lambda\|_{\Gamma_i}.$$

*Proof.* We first show that

$$r_i = \overline{\lambda}_i := \begin{cases} |\Omega_i|^{-1} (\lambda_i, 1)_{\Gamma_i}, & i \in I_{int}, \\ 0, & i \notin I_{int}. \end{cases}$$

If  $i \notin I_{int}$ , this follows by the definition of  $S_H$  since we then have  $r_i = \overline{\lambda}_i = 0$ . If  $i \in I_{int}$ , we set  $w_{h,i} = 1$  in (3.13b):

$$(r_i - \overline{\lambda}_i, 1)_{\Omega_i} = (\nabla \cdot \mathcal{R}_{h,i}\lambda, 1)_{\Omega_i} - (\overline{\lambda}_i, 1)_{\Omega_i} = (\mathcal{Q}_{h,i}\lambda - \lambda_i, 1)_{\Gamma_i} = 0 \quad \forall i \in I_{int},$$

using (3.9) and (3.11) in the final equality. Now (3.13b) implies that  $\nabla \cdot \mathcal{R}_{h,i} \lambda = \overline{\lambda}_i$ . Since this is a square, finite-dimensional linear system, uniqueness implies existence. Thus, we set  $\lambda = 0$  and note that  $r_i = \lambda_i = 0$ . In addition,  $\mathcal{Q}_{h,i}\lambda = 0$ , thus  $\mathcal{R}_{h,i}\lambda \in V_{h,i}^0$ . Setting test functions  $(\mathcal{R}_{h,i}\lambda, p_{h,i}^{\lambda})$  in the first two equations and summing them gives  $\mathcal{R}_{h,i}\lambda = 0$ . Finally, we use (3.5a) to derive that  $W_{h,i} = \nabla \cdot V_{h,i}^0 \oplus S_{H,i}$  which implies  $p_{h,i}^{\lambda} = 0$ , using (3.13a) and (3.13c).

We continue with the stability estimate by first obtaining a bound on the auxiliary variable  $p_{h,i}^{\lambda}$ . Recall that the discrete pair  $V_{h,i} \times W_{h,i}$  is stable (see (3.5b)), and note that  $p_{h,i}^{\lambda}$  has zero mean for  $i \in I_{int}$ . Thus, there exists  $\mathbf{v}_{h,p,i}^{0} \in V_{h,i}^{0}$  such that

$$\nabla \cdot \boldsymbol{v}_{h,p,i}^0 = p_{h,i}^{\lambda} \text{ in } \Omega_i, \quad \|\boldsymbol{v}_{h,p,i}^0\|_{\operatorname{div},\Omega_i} \lesssim \|p_{h,i}^{\lambda}\|_{\Omega_i}.$$

Using  $\boldsymbol{v}_{h,p,i}^{0}$  as a test function in (3.13a), we derive

$$\|p_{h,i}^{\lambda}\|_{\Omega_{i}}^{2} = \left(K^{-1}\mathcal{R}_{h,i}\lambda, \mathbf{v}_{h,p,i}^{0}\right)_{\Omega_{i}} \leq \|K^{-1}\mathcal{R}_{h,i}\lambda\|_{\Omega_{i}}\|\mathbf{v}_{h,p,i}^{0}\|_{\Omega_{i}} \lesssim \|\mathcal{R}_{h,i}\lambda\|_{\Omega_{i}}\|p_{h,i}^{\lambda}\|_{\Omega_{i}},$$

implying

Second, we note that  $\nabla \cdot \mathcal{R}_{h,i}\lambda = 0 \ \forall i \notin I_{int} \text{ since } \overline{\lambda}_i = 0$ . For the remaining indexes, i.e.,  $i \in I_{int}$ , we derive

(3.16a)

$$\|\nabla \cdot \mathcal{R}_{h,i}\lambda\|_{\Omega_i} = \|\overline{\lambda}_i\|_{\Omega_i} = |\Omega_i|^{-1/2}(\lambda,1)_{\Gamma_i} = |\Omega_i|^{-1/2}(\mathcal{Q}_{h,i}\lambda,1)_{\Gamma_i} \lesssim \|\mathcal{Q}_{h,i}\lambda\|_{\Gamma_i}.$$

Third, we introduce the discrete  $H(\operatorname{div}, \Omega_i)$ -extension operator from [32, sect. 4.1.2], and denote it by  $\mathcal{R}_{h,i}^{\star}: V_{h,i}^{\Gamma} \to V_{h,i}$ . This extension satisfies, for  $\psi_{h,i} \in V_{h,i}^{\Gamma}$ ,

$$\boldsymbol{\nu}_i \cdot \mathcal{R}_{h,i}^{\star} \psi_{h,i} = \psi_{h,i} \text{ on } \Gamma_i, \quad \boldsymbol{\nu}_i \cdot \mathcal{R}_{h,i}^{\star} \psi_{h,i} = 0 \text{ on } \partial \Omega_i \setminus \Gamma_i, \quad \|\mathcal{R}_{h,i}^{\star} \psi_{h,i}\|_{\operatorname{div},\Omega_i} \lesssim \|\psi_{h,i}\|_{\Gamma_i}.$$

The next step is to set the test functions  $\mathbf{v}_{h,i}^0 = \mathcal{R}_{h,i}\lambda - \mathcal{R}_{h,i}^{\star}(\mathcal{Q}_{h,i}\lambda)$ ,  $w_{h,i} = p_{h,i}^{\lambda}$ , and  $s_i = r_i$  in (3.13). After summation of the equations, we have

$$(K^{-1}\mathcal{R}_{h,i}\lambda,\mathcal{R}_{h,i}\lambda-\mathcal{R}_{h,i}^{\star}(\mathcal{Q}_{h,i}\lambda))_{\Omega_{i}}+(\nabla\cdot\mathcal{R}_{h,i}^{\star}(\mathcal{Q}_{h,i}\lambda),p_{h,i}^{\lambda})_{\Omega_{i}}=0.$$

Using bound (3.15) and the continuity bound for  $\|\mathcal{R}_{h,i}^{\star}(\mathcal{Q}_{h,i}\lambda)\|_{\operatorname{div},\Omega_i}$ , we obtain

$$\|\mathcal{R}_{h,i}\lambda\|_{\Omega_i}^2 \lesssim (\|\mathcal{R}_{h,i}\lambda\|_{\Omega_i} + \|p_{h,i}^{\lambda}\|_{\Omega_i})\|\mathcal{R}_{h,i}^{\star}(\mathcal{Q}_{h,i}\lambda)\|_{\operatorname{div},\Omega_i} \lesssim \|\mathcal{R}_{h,i}\lambda\|_{\Omega_i}\|\mathcal{Q}_{h,i}\lambda\|_{\Gamma_i},$$

which implies

(3.16b) 
$$\|\mathcal{R}_{h,i}\lambda\|_{\Omega_i} \lesssim \|\mathcal{Q}_{h,i}\lambda\|_{\Gamma_i}.$$

Collecting (3.16) and using that  $\|Q_{h,i}\lambda\|_{\Gamma_i} \lesssim \|\lambda\|_{\Gamma_i}$ , since both variants are generated using an  $L^2$ -projection, proves the stability estimate.

**3.2.** Well-posedness. In this section, we establish existence, uniqueness, and stability of the solution to the discrete problem (3.7) by showing that the assumptions from section 2.4 hold within this setting.

LEMMA 3.4 (A2). The bilinear forms  $a(\cdot,\cdot)$  and  $b(\cdot,\cdot)$  satisfy bounds (2.11).

*Proof.* Bounds (2.11a) and (2.11b) describe the continuity of the bilinear forms. These follow directly from the Cauchy–Schwarz inequality and the boundedness of K; cf. (3.2). Bound (2.11c) concerns coercivity. Recall that  $\nabla \cdot V_{h,i} \subseteq W_{h,i}$  from (3.5a) and that  $V_h \subseteq \bigoplus_i V_{h,i}$ . In turn, the assumption  $b(\boldsymbol{v}_h, w_h) = 0 \ \forall w_h \in W_h$  implies that  $\nabla \cdot \boldsymbol{v}_{h,i} = 0 \ \forall i$ . Using this in combination with (3.2) gives

$$a(\mathbf{v}_h, \mathbf{v}_h) = \|K^{-1/2}\mathbf{v}_h\|_{\Omega}^2 \gtrsim \|\mathbf{v}_h\|_{\Omega}^2 = \|\mathbf{v}_h\|_V^2.$$

Finally, inequality (2.11d) describes the discrete inf-sup condition. Let  $w_h \in W_h$  be given. Consider a global divergence problem on  $\Omega$ :

(3.17) 
$$\nabla \cdot \boldsymbol{v}^w = w_h \text{ in } \Omega, \quad \boldsymbol{v}^w = \boldsymbol{g}^w \text{ on } \partial \Omega,$$

where  $\boldsymbol{g}^w \in H^{1/2}(\partial\Omega)$  is such that  $(\boldsymbol{\nu} \cdot \boldsymbol{g}^w, 1)_{\partial\Omega} = (w_h, 1)_{\Omega}$  and  $\|\boldsymbol{g}^w\|_{\frac{1}{2},\partial\Omega} \lesssim \|w_h\|_{\Omega}$ . This problem has a solution  $\boldsymbol{v}^w \in (H^1(\Omega))^n$  satisfying [16]:

$$\|\boldsymbol{v}^w\|_{1,\Omega} \lesssim \|\boldsymbol{w}_h\|_{\Omega} + \|\boldsymbol{g}^w\|_{\frac{1}{2},\partial\Omega} \lesssim \|\boldsymbol{w}_h\|_{\Omega}.$$

Let  $\mu_h \in \Lambda_h$  be defined on each interface  $\Gamma_{ij}$  as the mean value of  $\boldsymbol{\nu} \cdot \boldsymbol{v}^w$ . We have

$$\|\mu_h\|_{\Gamma} \lesssim \sum_{i \in I_{\Omega}} \|\mu_{h,i}\|_{\Gamma_i} \lesssim \sum_{i \in I_{\Omega}} \|\boldsymbol{\nu}_i \cdot \boldsymbol{v}^w\|_{\Gamma_i} \lesssim \sum_{i \in I_{\Omega}} \|\boldsymbol{v}^w\|_{1,\Omega_i} \lesssim \|w_h\|_{\Omega}.$$

Moreover, on each interior subdomain  $\Omega_i$ , i.e., with  $\Gamma_i = \partial \Omega_i$ , we have that

$$(\mu_{h,i},1)_{\partial\Omega_i}=(\boldsymbol{\nu}_i\cdot\boldsymbol{v}^w,1)_{\partial\Omega_i}=(\nabla\cdot\boldsymbol{v}^w,1)_{\Omega_i}=(w_{h,i},1)_{\Omega_i}.$$

Consider the extension  $\mathcal{R}_{h,i}\mu_h$  and note that on each interior subdomain  $\Omega_i$ ,

$$(w_{h,i} - \nabla \cdot \mathcal{R}_{h,i}\mu_h, 1)_{\Omega_i} = (w_{h,i}, 1)_{\Omega_i} - (\boldsymbol{\nu}_i \cdot \mathcal{R}_{h,i}\mu_h, 1)_{\partial\Omega_i}$$
$$= (w_{h,i}, 1)_{\Omega_i} - (\mu_{h,i}, 1)_{\partial\Omega_i} = 0.$$

Then, the local discrete inf-sup condition (3.5b) implies that in each  $\Omega_i$  there exists  $\boldsymbol{v}_{h,i}^0 \in V_{h,i}^0$  such that

$$\nabla \cdot \boldsymbol{v}_{h,i}^0 = w_{h,i} - \nabla \cdot \mathcal{R}_{h,i} \mu_h$$
 in  $\Omega_i$ ,

and, using Lemma 3.3.

$$\begin{split} \sum_{i \in I_{\Omega}} \|\boldsymbol{v}_{h,i}^{0}\|_{\operatorname{div},\Omega_{i}} \lesssim \sum_{i \in I_{\Omega}} \|w_{h,i} - \nabla \cdot \mathcal{R}_{h,i}\mu_{h}\|_{\Omega_{i}} &\leq \sum_{i \in I_{\Omega}} (\|w_{h,i}\|_{\Omega_{i}} + \|\nabla \cdot \mathcal{R}_{h,i}\mu_{h}\|_{\Omega_{i}}) \\ \lesssim \sum_{i \in I_{\Omega}} (\|w_{h,i}\|_{\Omega_{i}} + \|\mu_{h,i}\|_{\Gamma_{i}}) \lesssim \|w_{h}\|_{\Omega}. \end{split}$$

The final step is to define  $\boldsymbol{v}_h^0 \in V_h^0$  such that  $\boldsymbol{v}_h^0|_{\Omega_i} := \boldsymbol{v}_{h,i}^0$ , set  $\boldsymbol{v}_h := \boldsymbol{v}_h^0 + \mathcal{R}_h \mu_h \in V_h$ , and note that

(3.18a) 
$$b(\mathbf{v}_h, w_h) = (\nabla \cdot (\mathbf{v}_h^0 + \mathcal{R}_h \mu_h), w_h)_{\Omega} = ||w_h||_W^2,$$

Combining equations (3.18) yields (2.11d).

Lemma 3.5 (A4). It holds that

$$(3.19) \forall i \in I_{\Omega}, \quad \|\boldsymbol{\nu}_{i} \cdot \boldsymbol{v}_{h,i}\|_{\Gamma_{i}} \lesssim h^{-1/2} \|\boldsymbol{v}_{h,i}\|_{\Omega_{i}} \quad \forall \boldsymbol{v}_{h,i} \in V_{h,i}.$$

*Proof.* The proof follows from a simple scaling argument.

We are now ready to establish the well-posedness of the flux-mortar mixed finite element method for the Darcy problem.

THEOREM 3.6. Problem (3.7) with  $\mathcal{R}_h^{\flat}$  or  $\mathcal{R}_h^{\sharp}$  from (3.13) admits a unique solution  $(\boldsymbol{u}_h, p_h) \in V_h^{\flat} \times W_h$  or  $V_h^{\sharp} \times W_h$ , respectively. In both cases, it holds that

$$||u_h||_V + ||p_h||_W \lesssim ||f||_{\Omega}.$$

Moreover, if the mortar condition A3 holds for the corresponding projection  $Q_h$ , then the mortar solution  $\lambda_h \in \Lambda_h$  is unique.

*Proof.* We follow the assumptions of Theorem 2.1. A1 is shown in Lemma 3.3 and A2 in Lemma 3.4. In turn, Theorem 2.1 ensures uniqueness of  $(\boldsymbol{u}_h, p_h)$  and the stability estimate (3.20) in both cases. Next, with A3 and A4, shown in Lemma 3.5, the application of Theorem 2.2 ensures the uniqueness of  $\lambda_h$ .

**3.3. Interpolation operators.** One of the main tools in deriving the error estimates is the construction of an appropriate interpolant associated with the discrete space  $V_h$ . The building blocks in our construction are the canonical interpolation operators associated with the subdomain finite element spaces  $V_{h,i}$ , namely  $\Pi_i^V: V_i \cap (H^{\epsilon}(\Omega_i))^n \to V_{h,i}$  with  $\epsilon > 0$ , with the properties

$$(3.21) \qquad \left(\nabla \cdot \left(\boldsymbol{v}_{i} - \Pi_{i}^{V} \boldsymbol{v}_{i}\right), w_{h,i}\right)_{\Omega_{i}} = 0 \qquad \forall w_{h,i} \in W_{h,i},$$

$$(3.22) \qquad \left(\boldsymbol{\nu}_{i} \cdot \left(\boldsymbol{v}_{i} - \boldsymbol{\Pi}_{i}^{V} \boldsymbol{v}_{i}\right), w_{h,i}\right)_{\partial \Omega_{i}} = 0 \qquad \forall w_{h,i} \in W_{h,i}.$$

In addition, let  $\Pi_i^W: L^2(\Omega_i) \to W_{h,i}$  and  $\Pi_{ij}^{\Lambda}: L^2(\Gamma_{ij}) \to \Lambda_{h,ij}$  denote the  $L^2$ -projection operators onto  $W_{h,i}$  and  $\Lambda_{h,ij}$ , respectively. Together with the projection  $\mathcal{Q}_{h,i}^{\flat}$  onto  $V_{h,i}^{\Gamma}$  introduced earlier, we recall the approximation properties [9]:

(3.23a) 
$$\| \boldsymbol{v} - \Pi_i^V \boldsymbol{v} \|_{\Omega_i} \lesssim h^{r_v} \| \boldsymbol{v} \|_{r_v, \Omega_i}, \qquad 0 < r_v \le k_v + 1$$

(3.23c) 
$$||w - \Pi_i^W w||_{\Omega_i} \lesssim h^{r_w} ||w||_{r_w, \Omega_i}, \qquad 0 \le r_w \le k_w + 1,$$

(3.23d) 
$$\|\mu - \Pi_{ij}^{\Lambda}\mu\|_{\Gamma_{ij}} \lesssim h_{\Gamma}^{r_{\Lambda}}\|\mu\|_{r_{\Lambda},\Gamma_{ij}}, \qquad 0 \leq r_{\Lambda} \leq k_{\Lambda} + 1,$$

(3.23e) 
$$\|\mu - \mathcal{Q}_{h,i}^{\flat}\mu\|_{\Gamma_{ij}} \lesssim h^{r_v} \|\mu\|_{r_v,\Gamma_{ij}}, \qquad 0 \leq r_v \leq k_v + 1.$$

The constants  $k_v$ ,  $k_w$ , and  $k_\Lambda$  represent the polynomial order of the spaces  $V_h$ ,  $W_h$ , and  $\Lambda_h$ , respectively, and  $i, j \in I_\Omega$ . To exemplify, we present two choices of stable mixed finite element pairs. For the pair of Raviart–Thomas of order  $k_v$  and discontinuous Lagrange elements of order  $k_w$ , we have  $k_v = k_w$ . On the other hand, choosing the Brezzi–Douglas–Marini elements of order  $k_v$  with discontinuous Lagrange elements of polynomial order  $k_w$ , we obtain a stable pair if  $k_v = k_w + 1$ . For more examples of stable finite element pairs, we refer the reader to [9, Chapter 2].

Let  $\Pi^W: W \to W_h$  and  $\Pi^{\Lambda}: \Lambda \to \Lambda_h$  be defined as the  $L^2$ -projections  $\Pi^W:=\bigoplus_i \Pi_i^W$  and  $\Pi^{\Lambda}:=\bigoplus_{i< j} \Pi_{ij}^{\Lambda}$ . The approximation properties of these operators follow directly from (3.23).

Next, we introduce the composite interpolant  $\Pi^V : \overline{V} \to V_h$ , where  $\overline{V} = \{ \boldsymbol{v} \in V : \boldsymbol{v}|_{\Omega_i} \in (H^{\epsilon}(\Omega_i))^n \text{ and } (\boldsymbol{\nu} \cdot \boldsymbol{u})|_{\Gamma} \in \Lambda \}$  with  $\epsilon > 0$ . Given  $\boldsymbol{u} \in \overline{V}$  with normal trace  $\lambda := (\boldsymbol{\nu} \cdot \boldsymbol{u})|_{\Gamma} \in \Lambda$ , we define  $\Pi^V \boldsymbol{u} \in V_h$  as

$$(3.24a) \qquad \Pi_{\flat}^{V} \boldsymbol{u} := \mathcal{R}_{h}^{\flat} \Pi^{\Lambda} \lambda + \bigoplus_{i} \Pi_{i}^{V} (\boldsymbol{u}_{i} - \mathcal{R}_{h,i}^{\flat} \lambda) = \mathcal{R}_{h}^{\flat} (\Pi^{\Lambda} \lambda - \lambda) + \bigoplus_{i} \Pi_{i}^{V} \boldsymbol{u}_{i},$$

$$(3.24b) \qquad \Pi_{\sharp}^{V} \boldsymbol{u} := \mathcal{R}_{h}^{\sharp} \Pi^{\Lambda} \lambda + \bigoplus_{i} \Pi_{i}^{V} (\boldsymbol{u}_{i} - \mathcal{R}_{h,i}^{\flat} \lambda) = \Pi_{\flat}^{V} \boldsymbol{u} + \mathcal{R}_{h}^{\sharp} \Pi^{\Lambda} \lambda - \mathcal{R}_{h}^{\flat} \Pi^{\Lambda} \lambda.$$

We note that (3.13d) for  $\mathcal{R}_{h,i}^{\flat}\lambda$  and (3.22) imply  $\boldsymbol{\nu}_{i}\cdot\Pi_{i}^{V}(\boldsymbol{u}_{i}-\mathcal{R}_{h,i}^{\flat}\lambda)=\mathcal{Q}_{h,i}^{\flat}\lambda-\mathcal{Q}_{h,i}^{\flat}\lambda=0$ , so (3.24) gives  $\Pi_{\flat}^{V}\boldsymbol{u}\in V_{h}^{\flat}$  and  $\Pi_{\sharp}^{V}\boldsymbol{u}\in V_{h}^{\sharp}$ . In the following, the use of  $\Pi^{V}$  indicates that the result is valid for both choices. We emphasize that the definitions of  $\Pi^{V}\boldsymbol{u}$  and  $\boldsymbol{u}_{h}$ , combined with (3.13d), imply

$$(3.25) \boldsymbol{\nu}_i \cdot \boldsymbol{\Pi}^V \boldsymbol{u} = \boldsymbol{\nu}_i \cdot \mathcal{R}_{h,i} \boldsymbol{\Pi}^{\Lambda} \boldsymbol{\lambda} = \mathcal{Q}_{h,i} \boldsymbol{\Pi}^{\Lambda} \boldsymbol{\lambda}, \quad \boldsymbol{\nu}_i \cdot \boldsymbol{u}_h = \boldsymbol{\nu}_i \cdot \mathcal{R}_{h,i} \boldsymbol{\lambda}_h = \mathcal{Q}_{h,i} \boldsymbol{\lambda}_h.$$

Lemma 3.7 (A5). The interpolation operator  $\Pi^V$  satisfies

$$(3.26) b(\boldsymbol{u} - \Pi^{V} \boldsymbol{u}, w_h) = 0 \forall w_h \in W_h.$$

*Proof.* In the case of  $\Pi_{\flat}^{V}$ , we first note that, due to (3.14),  $\nabla \cdot \mathcal{R}_{h,i}^{\flat}(\Pi^{\Lambda}\lambda - \lambda) = \overline{\Pi^{\Lambda}\lambda_{i}} - \overline{\lambda}_{i} = 0$ . Then the statement of the lemma follows from (3.21). In the case of  $\Pi_{\sharp}^{V}$ , due to (3.14),  $\nabla \cdot (\mathcal{R}_{h,i}^{\sharp}\Pi^{\Lambda}\lambda - \mathcal{R}_{h,i}^{\flat}\Pi^{\Lambda}\lambda) = 0$ , and the result follows.

We proceed with the approximation properties of the interpolants  $\Pi_{\flat}^{V}$  and  $\Pi_{\flat}^{V}$ .

Lemma 3.8. Assuming that u has sufficient regularity, then

$$(3.27a) \quad \|\boldsymbol{u} - \boldsymbol{\Pi}_{\flat}^{V} \boldsymbol{u}\|_{V} \lesssim h^{r_{v}} \sum_{i} \|\boldsymbol{u}\|_{r_{v},\Omega_{i}} + h^{r_{w}} \sum_{i} \|\nabla \cdot \boldsymbol{u}\|_{r_{w},\Omega_{i}} + h^{r_{\Lambda}}_{\Gamma} \sum_{i < j} \|\lambda\|_{r_{\Lambda},\Gamma_{ij}},$$

$$(3.27b) \| \boldsymbol{u} - \Pi_{\sharp}^{V} \boldsymbol{u} \|_{V} \lesssim h^{r_{v}} \sum_{i} \| \boldsymbol{u} \|_{r_{v},\Omega_{i}} + h^{r_{w}} \sum_{i} \| \nabla \cdot \boldsymbol{u} \|_{r_{w},\Omega_{i}} + h_{\Gamma}^{r_{\Lambda}} \sum_{i < j} \| \lambda \|_{r_{\Lambda},\Gamma_{ij}} + h^{\tilde{r}_{v}} \sum_{i < j} \| \lambda \|_{\tilde{r}_{v},\Gamma_{ij}}$$

for 
$$0 < r_v \le k_v + 1$$
,  $0 \le r_w \le k_w + 1$ ,  $0 \le r_\Lambda \le k_\Lambda + 1$ , and  $0 \le \tilde{r}_v \le k_v + 1$ .

Proof. Using (3.24a), bound (3.27a) for  $\Pi_{\flat}^{V}$  follows from (3.14) and the approximation bounds (3.23a), (3.23b), and (3.23d). For  $\Pi_{\sharp}^{V}$ , using (3.24b), we need to bound  $\|\mathcal{R}_{h,i}^{\sharp}\Pi^{\Lambda}\lambda - \mathcal{R}_{h,i}^{\flat}\Pi^{\Lambda}\lambda\|_{\operatorname{div},\Omega_{i}}$ . Since this is the extension that solves (3.13) with boundary data  $\mathcal{Q}_{h,i}^{\sharp}\Pi^{\Lambda}\lambda - \mathcal{Q}_{h,i}^{\flat}\Pi^{\Lambda}\lambda$ , we have  $\mathcal{R}_{h,i}^{\sharp}\Pi^{\Lambda}\lambda - \mathcal{R}_{h,i}^{\flat}\Pi^{\Lambda}\lambda = \mathcal{R}_{h,i}^{\flat}(\mathcal{Q}_{h,i}^{\sharp}\Pi^{\Lambda}\lambda - \mathcal{Q}_{h,i}^{\flat}\Pi^{\Lambda}\lambda)$ . We use this observation in combination with (3.14) to obtain the bound

$$\begin{split} &\|\mathcal{R}_{h,i}^{\sharp}\Pi^{\Lambda}\lambda - \mathcal{R}_{h,i}^{\flat}\Pi^{\Lambda}\lambda\|_{\operatorname{div},\Omega_{i}} \lesssim \|\mathcal{Q}_{h,i}^{\sharp}\Pi^{\Lambda}\lambda - \mathcal{Q}_{h,i}^{\flat}\Pi^{\Lambda}\lambda\|_{\Gamma_{i}} \\ &\leq \|\mathcal{Q}_{h,i}^{\sharp}\Pi^{\Lambda}\lambda - \mathcal{Q}_{h,i}^{\sharp}\lambda\|_{\Gamma_{i}} + \|\mathcal{Q}_{h,i}^{\sharp}\lambda - \mathcal{Q}_{h,i}^{\flat}\lambda\|_{\Gamma_{i}} + \|\mathcal{Q}_{h,i}^{\flat}\Pi^{\Lambda}\lambda - \mathcal{Q}_{h,i}^{\flat}\lambda\|_{\Gamma_{i}} \\ &\leq 2\|\Pi^{\Lambda}\lambda - \lambda\|_{\Gamma_{i}} + \|\mathcal{Q}_{h,i}^{\sharp}\lambda - \mathcal{Q}_{h,i}^{\flat}\lambda\|_{\Gamma_{i}}. \end{split}$$

In order to bound the final term, we use [4, Lemma 3.2], which states that if A3 holds for  $\mathcal{Q}_h^{\flat}$ , then

$$(3.28) \qquad \sum_{i < j} \|\mathcal{Q}_{h,i}^{\sharp} \lambda - \mathcal{Q}_{h,i}^{\flat} \lambda\|_{\Gamma_{ij}} \lesssim h^{\tilde{r}_v} \sum_{i < j} \|\lambda\|_{\tilde{r}_v, \Gamma_{ij}}, \qquad 0 \le \tilde{r}_v \le k_v + 1.$$

The proof of (3.27b) is completed by using (3.23d) and (3.28).

**3.4. Error estimates.** We now turn to the a priori error analysis. By Lemma 3.7, assumption A5 is satisfied and we therefore invoke Theorem 2.3 to obtain the a priori error estimate (2.14). Thus, to complete the error estimate, we need to derive a bound on the consistency error  $\mathcal{E}_c$ . Before we do that, we remark that, since  $\nabla \cdot V_{h,i} = W_{h,i}$  (cf. (3.5a)), we can obtain a standalone bound for  $\nabla \cdot (\boldsymbol{u} - \boldsymbol{u}_h)$ . In particular, the error equation (2.16b) implies that  $\nabla \cdot (\Pi^V \boldsymbol{u} - \boldsymbol{u}_h) = 0$  in  $\Omega_i$ ; therefore, using (3.26),

(3.29) 
$$\nabla \cdot (\boldsymbol{u} - \boldsymbol{u}_h) = \nabla \cdot (\boldsymbol{u} - \Pi^V \boldsymbol{u}) = \nabla \cdot \boldsymbol{u} - \Pi_i^W (\nabla \cdot \boldsymbol{u}) = f - \Pi_i^W f \text{ in } \Omega_i,$$

which is simply the approximation error of the source term f in  $W_h$ .

The next step is to derive a bound on the consistency error  $\mathcal{E}_c$ . For that, we recall its definition (2.15) and apply integration by parts on each  $\Omega_i$  with p = 0 on  $\partial\Omega$ :

(3.30) 
$$\mathcal{E}_{c} = \sup_{\boldsymbol{v}_{h} \in V_{h}} \|\boldsymbol{v}_{h}\|_{V}^{-1} \Big( (K^{-1}\boldsymbol{u}, \boldsymbol{v}_{h})_{\Omega} - \sum_{i} (p, \nabla \cdot \boldsymbol{v}_{h})_{\Omega_{i}} \Big)$$
$$= \sup_{\boldsymbol{v}_{h} \in V_{h}} \|\boldsymbol{v}_{h}\|_{V}^{-1} \sum_{i} -(p, \boldsymbol{\nu}_{i} \cdot \boldsymbol{v}_{h, i})_{\Gamma_{i}}.$$

In the last equality we used that  $K^{-1}u = -\nabla p$  from (3.1).

We continue the derivation using arguments that depend on the choice of extension operator, as outlined in the following two subsections.

**3.4.1. Consistency error using**  $\mathcal{R}_h^{\sharp}$ . For this choice of extension operator (cf. section 3.1.2), we use the weak continuity from Lemma 3.2 to bound the consistency error (3.30). Let the discrete subspace consisting of continuous mortar functions be denoted by  $\Lambda_{h,c} \subset \Lambda_h$ . Next, let  $\Pi_c^{\Lambda}: H^1(\Gamma) \to \Lambda_{h,c}$  be the Scott–Zhang interpolant [34] into  $\Lambda_{h,c}$ . This interpolant has the approximation property

$$(3.31) ||p - \Pi_c^{\Lambda} p||_{s_{\Lambda}, \Gamma} \lesssim h_{\Gamma}^{r_{\Lambda} - s_{\Lambda}} ||p||_{r_{\Lambda}, \Gamma}, \quad 1 \leq r_{\Lambda} \leq k_{\Lambda} + 1, \ 0 \leq s_{\Lambda} \leq 1.$$

Importantly, the Scott–Zhang interpolant can be constructed to use only trace values on  $\partial\Gamma$ . Recalling that p=0 on  $\partial\Omega$ , this implies that  $(I-\Pi_c^{\Lambda})p=0$  on  $\partial\Gamma$ . This allows us to extend it continuously by zero on  $\partial\Omega$  and we let  $E_0(I-\Pi_c^{\Lambda})p$  denote the extended function. On each subdomain  $\Omega_i$ , it satisfies  $||E_0(I-\Pi_c^{\Lambda})p||_{\frac{1}{2},\Omega_i} \lesssim ||(I-\Pi_c^{\Lambda})p||_{\frac{1}{2},\Gamma_i}$ .

Recall that  $\mathbf{v}_h \in V_h^{\sharp}$  is weakly continuous due to Lemma 3.2. Consequently,  $\sum_i (\Pi_c^{\Lambda} p, \boldsymbol{\nu}_i \cdot \mathbf{v}_{h,i})_{\Gamma_i} = 0$  and we use this to derive

$$\sum_{i} (p, \boldsymbol{\nu}_{i} \cdot \boldsymbol{v}_{h,i})_{\Gamma_{i}} = \sum_{i} ((I - \Pi_{c}^{\Lambda})p, \boldsymbol{\nu}_{i} \cdot \boldsymbol{v}_{h,i})_{\Gamma_{i}} = \sum_{i} (E_{0}(I - \Pi_{c}^{\Lambda})p, \boldsymbol{\nu}_{i} \cdot \boldsymbol{v}_{h,i})_{\partial\Omega_{i}}$$

$$\lesssim \sum_{i} \|E_{0}(I - \Pi_{c}^{\Lambda})p\|_{\frac{1}{2},\partial\Omega_{i}} \|\boldsymbol{v}_{h,i}\|_{\operatorname{div},\Omega_{i}} \lesssim \|(I - \Pi_{c}^{\Lambda})p\|_{\frac{1}{2},\Gamma} \|\boldsymbol{v}_{h}\|_{V},$$
3.32)

where we used the normal trace inequality  $\|\boldsymbol{\nu}_i \cdot \boldsymbol{v}_{h,i}\|_{-\frac{1}{2},\partial\Omega_i} \lesssim \|\boldsymbol{v}_{h,i}\|_{\operatorname{div},\Omega_i}$  [9]. This gives a bound on the consistency error  $\mathcal{E}_c$  from (3.30). We arrive at the main result of this subsection.

Theorem 3.9. Let  $\mathcal{R}_h = \mathcal{R}_h^{\sharp}$ . If A3 holds for  $\mathcal{Q}_h^{\flat}$  and the solution is sufficiently regular, then

$$\|\boldsymbol{u} - \boldsymbol{u}_h\|_V + \|p - p_h\|_W$$

$$\lesssim h^{k_{v}+1} \left( \sum_{i} \|\boldsymbol{u}\|_{k_{v}+1,\Omega_{i}} + \sum_{i < j} \|\lambda\|_{k_{v}+1,\Gamma_{ij}} \right)$$

$$+ h^{k_{w}+1} \sum_{i} \left( \|\nabla \cdot \boldsymbol{u}\|_{k_{w}+1,\Omega_{i}} + \|p\|_{k_{w}+1,\Omega_{i}} \right) + h_{\Gamma}^{k_{\Lambda}+1} \sum_{i < j} \|\lambda\|_{k_{\Lambda}+1,\Gamma_{ij}} + h_{\Gamma}^{k_{\Lambda}+\frac{1}{2}} \|p\|_{k_{\Lambda}+1,\Gamma}.$$

*Proof.* Noting that assumption A5 has been verified in Lemma 3.7, we invoke Theorem 2.3. Bound (2.14), combined with (3.30) and (3.32), implies

$$\|\boldsymbol{u} - \boldsymbol{u}_h\|_V + \|p - p_h\|_W \lesssim \|\Pi_{\sharp}^V \boldsymbol{u} - \boldsymbol{u}\|_V + \|\Pi^W p - p\|_W + \|\Pi_c^{\Lambda} p - p\|_{\frac{1}{2}, \Gamma}.$$

The assertion of the theorem follows by combining the above bound with the approximation properties (3.23), (3.27b), and (3.31).

**3.4.2.** Consistency error using  $\mathcal{R}_h^{\flat}$ . For this choice of extension operator (cf. section 3.1.1), we require a different strategy to bound the consistency error (3.30) since weak continuity of normal traces in  $V_h^{\flat}$  is not guaranteed. We note that  $\boldsymbol{v}_h \in V_h^{\flat}$  can be decomposed as  $\boldsymbol{v}_h =: \boldsymbol{v}_h^0 + \mathcal{R}_h^{\flat} \mu_h$ , with  $(\boldsymbol{v}_h^0, \mu_h) \in V_h^0 \times \Lambda_h$ . Using that  $\mathcal{Q}_{h,i}^{\flat}$  is the  $L^2$ -projection onto  $V_{h,i}^{\Gamma}$  (cf. (3.8)) and that p is single-valued on  $\Gamma$ , we derive

$$\begin{split} \sum_{i} (p, \boldsymbol{\nu}_{i} \cdot \boldsymbol{v}_{h})_{\Gamma_{i}} &= \sum_{i} (p, \mathcal{Q}_{h,i}^{\flat} \mu_{h,i})_{\Gamma_{i}} = \sum_{i} (\mathcal{Q}_{h,i}^{\flat} p, \mu_{h,i})_{\Gamma_{i}} \\ &= \sum_{i} (\mathcal{Q}_{h,i}^{\flat} p - p, \mu_{h,i})_{\Gamma_{i}} \leq \sum_{i} \|\mathcal{Q}_{h,i}^{\flat} p - p\|_{\Gamma_{i}} \|\mu_{h,i}\|_{\Gamma_{i}}. \end{split}$$

We continue the bound using the mortar condition A3 and the trace inequality (3.19):

$$\sum_{i} (p, \boldsymbol{\nu}_{i} \cdot \boldsymbol{v}_{h})_{\Gamma_{i}} \lesssim \sum_{i} \|\mathcal{Q}_{h,i}^{\flat} p - p\|_{\Gamma_{i}} \|\mathcal{Q}_{h,i}^{\flat} \mu_{h,i}\|_{\Gamma_{i}} = \sum_{i} \|\mathcal{Q}_{h,i}^{\flat} p - p\|_{\Gamma_{i}} \|\boldsymbol{\nu}_{i} \cdot \boldsymbol{v}_{h,i}\|_{\Gamma_{i}}$$

$$\lesssim \sum_{i} \|\mathcal{Q}_{h,i}^{\flat} p - p\|_{\Gamma_{i}} h^{-1/2} \|\boldsymbol{v}_{h,i}\|_{\Omega_{i}} \lesssim h^{-1/2} \sum_{i} \|\mathcal{Q}_{h,i}^{\flat} p - p\|_{\Gamma_{i}} \|\boldsymbol{v}_{h}\|_{V}.$$
(3.33)

This gives a bound on the consistency error  $\mathcal{E}_c$  from (3.30), which leads us to the main result of this subsection.

THEOREM 3.10. Let  $\mathcal{R}_h = \mathcal{R}_h^{\flat}$ . If A3 holds and the solution is sufficiently regular, then

$$\begin{aligned} \| \boldsymbol{u} - \boldsymbol{u}_h \|_V + \| p - p_h \|_W &\lesssim h^{k_v + 1} \sum_i \| \boldsymbol{u} \|_{k_v + 1, \Omega_i} + h_{\Gamma}^{k_{\Lambda} + 1} \sum_{i < j} \| \lambda \|_{k_{\Lambda} + 1, \Gamma_{ij}} \\ + h^{k_w + 1} \sum_i \left( \| \nabla \cdot \boldsymbol{u} \|_{k_w + 1, \Omega_i} + \| p \|_{k_w + 1, \Omega_i} \right) + h^{k_v + \frac{1}{2}} \sum_i \| p \|_{k_v + 1, \Gamma_i}. \end{aligned}$$

*Proof.* We again invoke Theorem 2.3. Bound (2.14), combined with (3.30) and (3.33), for which A3 is utilized, gives

$$\|\boldsymbol{u} - \boldsymbol{u}_h\|_V + \|p - p_h\|_W \lesssim \|\Pi_b^V \boldsymbol{u} - \boldsymbol{u}\|_V + \|\Pi^W p - p\|_W + h^{-1/2} \sum_i \|\mathcal{Q}_{h,i}^b p - p\|_{\Gamma_i}.$$

An application of (3.23) and (3.27a) completes the proof.

**3.4.3.** Comparison. The previous two sections indicate that theoretically the choice of extension operator affects the resulting discretization error. Most importantly, the estimates from Theorems 3.9 and 3.10 differ in the interface pressure terms

$$h_{\Gamma}^{k_{\Lambda}+1/2} ||p||_{k_{\Lambda}+1,\Gamma}$$
 versus  $h^{k_{v}+1/2} ||p||_{k_{v}+1,\Gamma}$ .

Both choices lead to a suboptimal convergence rate if  $k_{\Lambda} = k_v$ , i.e., if the polynomial orders of  $\Lambda_h$  and  $V_h$  are equal. This loss can be remediated in the case of the weakly continuous projection  $\mathcal{R}_h^{\sharp}$  by setting  $k_{\Lambda} > k_v$ , i.e., by choosing a higher order mortar space  $\Lambda_h$  within the limit of the mortar condition A3; cf. Remark 3.2. This behavior is similar to the pressure-mortar method [4, 5]. It is important to note, however, that the two projections behave numerically in a very similar way, as observed in section 5.

Remark 3.6. In the special case  $\Lambda_{h,i} \subseteq V_{h,i}^{\Gamma}$ , one can simply take  $Q_{h,i} = I$ . Then,

$$\sum_{i} (p, \boldsymbol{\nu}_i \cdot \boldsymbol{v}_h)_{\Gamma_i} = \sum_{i} (p, \mu_{h,i})_{\Gamma_i} = 0,$$

implying that  $\mathcal{E}_c = 0$  and there is no suboptimal term in the error bound.

**3.4.4.** The interface flux. The error estimates derived in the previous sections show convergence of the subdomain variables  $u_h$  and  $p_h$ . However, convergence of the mortar variable  $\lambda_h$  itself has not been obtained. We therefore devote this section to finding error estimates of the mortar variable for both types of projection operators. The results are presented in a general setting. However, we recall that the discrete solution  $(u_h, p_h) \in V_h \times W_h$  implicitly depends on the chosen projection operator.

In the following theorem we consider two measures of the interface flux error, comparing the true interface flux  $\lambda$  to either the mortar flux  $\lambda_h$  or to the normal trace of the velocity  $u_h$  on  $\Gamma$ ,  $\nu_i \cdot u_h = \mathcal{Q}_{h,i}\lambda_h$ .

THEOREM 3.11. If A3 holds and the solution is sufficiently regular, then

$$\begin{split} \|\lambda - \lambda_h\|_{\Gamma} &\lesssim h_{\Gamma}^{k_{\Lambda}+1} \sum_{i < j} \|\lambda\|_{k_{\Lambda}+1,\Gamma_{ij}} + h^{-1/2} (\|\Pi^{V} \boldsymbol{u} - \boldsymbol{u}\|_{V} + \mathcal{E}_{c}), \\ &\sum_{i} \|\lambda - \mathcal{Q}_{h,i} \lambda_h\|_{\Gamma_{i}} &\lesssim h_{\Gamma}^{k_{\Lambda}+1} \sum_{i < j} \|\lambda\|_{k_{\Lambda}+1,\Gamma_{ij}} + h^{-1/2} (\|\Pi^{V} \boldsymbol{u} - \boldsymbol{u}\|_{V} + \mathcal{E}_{c}) \\ &+ h^{k_{v}+1} \sum_{i < j} \|\lambda\|_{k_{v}+1,\Gamma_{ij}}. \end{split}$$

*Proof.* Using A3, (3.25), and the discrete trace inequality (3.19), we obtain

$$\|\lambda - \lambda_h\|_{\Gamma} \leq \|\lambda - \Pi^{\Lambda}\lambda\|_{\Gamma} + \|\Pi^{\Lambda}\lambda - \lambda_h\|_{\Gamma} \lesssim \|\lambda - \Pi^{\Lambda}\lambda\|_{\Gamma} + \sum_{i} \|\mathcal{Q}_{h,i}(\Pi^{\Lambda}\lambda - \lambda_h)\|_{\Gamma_{i}}$$

$$= \|\lambda - \Pi^{\Lambda}\lambda\|_{\Gamma} + \sum_{i} \|\boldsymbol{\nu}_{i} \cdot (\Pi^{V}\boldsymbol{u} - \boldsymbol{u}_{h})\|_{\Gamma_{i}}$$

$$\leq \|\lambda - \Pi^{\Lambda}\lambda\|_{\Gamma} + h^{-1/2}\|\Pi^{V}\boldsymbol{u} - \boldsymbol{u}_{h}\|_{V}.$$

$$(3.34)$$

The next step is to note that (3.5a) implies  $b(\mathbf{v}_h, \Pi^W p - p) = 0$ . In turn, the bound (2.20d) in Theorem 2.3 is obsolete and (2.21) can be improved to

$$\|\Pi^{V}\boldsymbol{u} - \boldsymbol{u}_{h}\|_{V} + \|\Pi^{W}\boldsymbol{p} - \boldsymbol{p}_{h}\|_{W} \lesssim \|\Pi^{V}\boldsymbol{u} - \boldsymbol{u}\|_{V} + \mathcal{E}_{c}.$$

Combining this with (3.34) and the approximation property (3.23d) then give us the first bound. The second bound follows from the triangle inequality,

$$\|\lambda - \mathcal{Q}_{h,i}\lambda_h\|_{\Gamma_i} \le \|\lambda - \mathcal{Q}_{h,i}\lambda\|_{\Gamma_i} + \|\mathcal{Q}_{h,i}(\lambda - \lambda_h)\|_{\Gamma_i} \le \|\lambda - \mathcal{Q}_{h,i}\lambda\|_{\Gamma_i} + \|\lambda - \lambda_h\|_{\Gamma_i},$$
and the use of the approximation property (3.23e).

Remark 3.7. The estimates from Theorem 3.11 can be further developed by invoking the approximation properties (3.23) and bounding the consistency error  $\mathcal{E}_c$  as in sections 3.4.1 and 3.4.2. In their presented form, however, these results emphasize that there is a half order reduction in convergence for the mortar variable compared to the velocity. Such reduction is expected, since we measure the mortar error in the  $L^2(\Gamma)$ -norm, rather than the  $H^{-1/2}(\Gamma)$ -norm.

**3.5. Interface problem.** By following the steps of section 2.5, the flux-mortar mixed finite element method can be reduced to an interface problem concerning only the mortar variable  $\lambda$ . In order to do so, we need to verify assumption A6.

LEMMA 3.12 (A6). The following inf-sup condition holds for the spaces  $\Lambda_h \times S_H$ :

$$\forall s_H \in S_H, \ \exists 0 \neq \mu_h \in \Lambda_h \ such \ that \ b(\mathcal{R}_h \mu_h, s_H) \gtrsim \|\mu_h\|_{\Lambda} \|s_H\|_W.$$

*Proof.* Setting  $w_h := s_H \in S_H \subseteq W_h$  in the proof of (2.11d) in Lemma 3.4 leads to a pair  $(\boldsymbol{v}_h^0, \mu_h)$  with  $\boldsymbol{v}_h^0 = 0$  that satisfies (3.18), i.e.,  $\|\mu_h\|_{\Lambda} \lesssim \|s_H\|_W$ , and  $b(\mathcal{R}_h \mu_h, s_H) = \|s_H\|_W^2.$ 

As noted in section 2.5, the interface problem (2.25) improves the solution with respect to (2.9b), which in this case is based on Darcy's law and enforces continuity of pressure. On the other hand, mass conservation is already ensured, locally, after solving (2.24) and the iterative solution of (2.25) effectively updates the velocity with divergence-free functions.

4. Stokes flow. As our next example, we consider Stokes flow and follow the steps from section 2 to formulate and analyze the corresponding flux-mortar mixed finite element method. The governing equations are

(4.1a) 
$$\sigma := \tilde{\mu}\varepsilon(\boldsymbol{u}) - pI \qquad \text{in } \Omega.$$

$$\begin{aligned} (4.1a) & \sigma := \tilde{\mu}\varepsilon(\boldsymbol{u}) - pI & & \text{in } \Omega, \\ (4.1b) & -\nabla \cdot \sigma = \boldsymbol{g}, & & \nabla \cdot \boldsymbol{u} = f & & \text{in } \Omega, \\ (4.1c) & & \boldsymbol{u} = 0 & \text{on } \partial_{\boldsymbol{u}}\Omega, & & \sigma \boldsymbol{\nu} = 0 & & \text{on } \partial_{\sigma}\Omega, \end{aligned}$$

(4.1c) 
$$\mathbf{u} = 0$$
 on  $\partial_{\mathbf{u}}\Omega$ ,  $\sigma \mathbf{v} = 0$  on  $\partial_{\sigma}\Omega$ .

Here,  $\tilde{\mu}$  represents the viscosity, g is a body force, f is the mass source, and  $\varepsilon$  denotes the symmetric gradient, i.e.,  $\varepsilon(\boldsymbol{v}) := \frac{1}{2}(\nabla \boldsymbol{v} + (\nabla \boldsymbol{v})^T)$ . Moreover,  $\partial_u \Omega \cup \partial_\sigma \Omega$  forms a disjoint decomposition of  $\partial\Omega$  with  $|\partial_u\tilde{\Omega}|>0$  and  $|\partial_\sigma\Omega|>0$ . For simplicity, we assume that the interface  $\Gamma$  only touches the boundary on  $\partial_{\mu}\Omega$ .

Let us continue by defining the function spaces  $V \times W$ :

$$V:=\left\{\boldsymbol{v}\in (H^1(\Omega))^n,\quad \boldsymbol{v}|_{\partial_u\Omega}=0\right\}, \qquad \qquad W:=L^2(\Omega).$$

The variational formulation of problem (4.1) obtains the form (2.1) by defining the bilinear forms:

$$(4.2) a_i(\boldsymbol{u}_i, \boldsymbol{v}_i) := (\tilde{\mu}\varepsilon(\boldsymbol{u}_i), \varepsilon(\boldsymbol{v}_i))_{\Omega_i}, b_i(\boldsymbol{u}_i, w_i) := (\nabla \cdot \boldsymbol{u}_i, w_i)_{\Omega_i}.$$

In line with (2.3), we let  $\operatorname{Tr}_i \mathbf{v}_i := \mathbf{v}_i|_{\Gamma_i}$  be the trace of all components of the vector function  $v_i \in V_i$  onto  $\Gamma_i$ . We define the trace space  $\Lambda := (H^{1/2}(\Gamma))^n$  and endow it with the norm  $\|\boldsymbol{\mu}\|_{\Lambda} := \sum_{i} \|\boldsymbol{\mu}_{i}\|_{\Lambda_{i}}$ , with

(4.3) 
$$\|\boldsymbol{\mu}_i\|_{\Lambda_i} := \left\{ \begin{array}{ll} \|\boldsymbol{\mu}_i\|_{\frac{1}{2},\partial\Omega_i}, & i \in I_{int}, \\ \|E_{i,0}\boldsymbol{\mu}_i\|_{\frac{1}{2},\partial\Omega_i}, & i \notin I_{int}, \end{array} \right.$$

where  $E_{i,0}$  is the extension by zero to  $\partial \Omega_i$ .

We end this subsection with a statement of a version of Korn's inequality [12, (1.8), which will be used to establish coercivity of the bilinear form  $a(\cdot,\cdot)$ . Let  $\mathcal{O} \subset \mathbb{R}^n$ , n=2,3, be a connected bounded domain and let  $\mathcal{G}$  with  $|\mathcal{G}|>0$  be a section of its boundary. Then,  $\forall v \in (H^1(\mathcal{O}))^n$ ,

(4.4) 
$$|\boldsymbol{v}|_{1,\mathcal{O}} \lesssim \left( \|\varepsilon(\boldsymbol{v})\|_{\mathcal{O}} + \sup_{\substack{\boldsymbol{m} \in \mathbf{RM}(\mathcal{O}) \\ \|\boldsymbol{m}\|_{\mathcal{G}} = 1, \, \int_{\mathcal{G}} \boldsymbol{m} \, ds = 0}} (\boldsymbol{v}, \boldsymbol{m})_{\mathcal{G}} \right),$$

where  $\mathbf{RM}(\mathcal{O})$  is the space of rigid body motions on  $\mathcal{O}$ . Combined with Poincaré inequality [32],  $\forall v \in (H^1(\mathcal{O}))^n$  with  $\int_{\mathcal{G}} v \, ds = 0$ ,  $\|v\|_{\mathcal{O}} \lesssim |v|_{1,\mathcal{O}}$ , (4.4) implies that  $\forall v \in (H^1(\mathcal{O}))^n \text{ with } (v, m)_{\mathcal{G}} = 0 \ \forall m \in \mathbf{RM}(\mathcal{O}),$ 

$$\|\boldsymbol{v}\|_{1,\mathcal{O}} \lesssim \|\varepsilon(\boldsymbol{v})\|_{\mathcal{O}}.$$

**4.1. Discretization.** For each  $i \in I_{\Omega}$ , we choose a finite element pair  $V_{h,i} \times W_{h,i} \subset V_i \times W_i$  such that it is stable for the Stokes subproblem on  $\Omega_{h,i}$ . Stable mixed finite element pairs for the Stokes subproblems (see, e.g., [9, Chapter 8]) include the Taylor–Hood pair, the MINI mixed finite element, and the Bernardi–Raugel pair. Note that the essential boundary condition  $\mathbf{u}_S = 0$  on  $\partial_u \Omega$  is built in  $V_{h,i}$ .

We next define the discrete flux space  $\Lambda_h \subset \Lambda$  by introducing a globally conforming shape-regular mesh on  $\Gamma$ . Such mesh can be obtained as the trace of a mesh  $\tilde{\Omega}_h$  on  $\Omega$  that is aligned with the domain decomposition. Let  $\tilde{V}_h \subset V|_{\Omega}$  be a conforming Lagrange finite element space on  $\tilde{\Omega}_h$ . We then define the discrete flux space on  $\Gamma$  as  $\Lambda_h := \operatorname{Tr} \tilde{V}_h$ .

Following definition (2.6), the space  $S_H$  is given by  $S_{H,i} = \mathbb{R}$  if  $\partial \Omega_i \cap \partial_\sigma \Omega = \emptyset$  and zero otherwise. Let  $W_{h,i}^0 := W_{h,i} \cap S_{H,i}^{\perp}$ . We emphasize that the stability of the finite element pair ensures the following inf-sup condition for each  $i \in I_{\Omega}$ :

$$(4.6) \quad \forall w_{h,i}^0 \in W_{h,i}^0, \ \exists \ 0 \neq \boldsymbol{v}_{h,i}^0 \in V_{h,i}^0 \text{ such that } b_i \left(\boldsymbol{v}_{h,i}^0, w_{h,i}^0\right) \gtrsim \|\boldsymbol{v}_{h,i}^0\|_{V_i} \|w_{h,i}^0\|_{W_i}.$$

We continue with the definition of the operator  $Q_{h,i}: \Lambda \to \operatorname{Tr}_i V_{h,i}$ . This operator needs to satisfy

$$(\boldsymbol{\nu}_i \cdot (\mathcal{Q}_{h,i}\boldsymbol{\lambda} - \boldsymbol{\lambda}), 1)_{\Gamma_i} = 0, \quad i \in I_{\Omega},$$

which is needed for inf-sup stability (cf. A2) and b-compatibility of the interpolant  $\Pi^V$  (cf. A5). The  $L^2$ -projection onto  $\operatorname{Tr}_i V_{h,i}$  does not satisfy (4.7), since the space  $\operatorname{Tr}_i V_{h,i}$  is continuous on  $\Gamma_i$ , but the normal vector  $\boldsymbol{\nu}_i$  is discontinuous at the corners of the subdomains. We therefore need a different construction. Let  $\mathcal{I}_{\Gamma_i}: \Lambda_i \to \operatorname{Tr}_i V_{h,i}$  be a suitable interpolant or projection with optimal approximation properties. Specific choices of  $\mathcal{I}_{\Gamma_i}$  will be discussed below. Since  $\mathcal{I}_{\Gamma_i}$  may not satisfy (4.7), we correct it on each flat face F of  $\Gamma_i$ . We assume that, given  $\boldsymbol{\lambda} \in \Lambda_i$ , there exists  $\boldsymbol{c}_{h,i}^F \in \operatorname{Tr}_i V_{h,i}|_F \cap (H_0^1(F))^n$  such that

$$(4.8) \quad \left(\boldsymbol{c}_{h,i}^{F}, \boldsymbol{\chi}_{h,i}\right)_{F} = (\boldsymbol{\lambda} - \mathcal{I}_{\Gamma_{i}}\boldsymbol{\lambda}, \boldsymbol{\chi}_{h,i})_{F} \quad \forall \boldsymbol{\chi}_{h,i} \in V_{h,i}^{F}, \quad \|\boldsymbol{c}_{h,i}^{F}\|_{\frac{1}{2},F} \lesssim \|\boldsymbol{\lambda} - \mathcal{I}_{\Gamma_{i}}\boldsymbol{\lambda}\|_{\frac{1}{2},F},$$

where  $V_{h,i}^F$  is a suitably defined finite element space on F such that  $\nu_i|_F \in V_{h,i}^F$ . We refer to [19, Appendix] for examples of spaces and constructions of  $\mathbf{c}_{h,i}^F$ . In particular, in two dimensions, assuming that  $\lambda \in \mathcal{C}^0(\Gamma_i)$ , we can take  $\mathcal{I}_{\Gamma_i}\lambda$  to be the Lagrange interpolant and use the constructions from [19, section 7.1]. Alternatively, in both two and three dimensions we can take  $\mathcal{I}_{\Gamma_i}$  to be the  $L^2$ -projection onto  $\operatorname{Tr}_i V_{h,i}$  and use the construction from [19, section 7.2]. We then define

$$\mathcal{Q}_{h,i}oldsymbol{\lambda} := \mathcal{I}_{\Gamma_i}oldsymbol{\lambda} + \sum_{F \subset \Gamma_i} oldsymbol{c}_{h,i}^F,$$

which satisfies for each face F,

$$(\mathcal{Q}_{h,i}\boldsymbol{\lambda} - \boldsymbol{\lambda}, \boldsymbol{\chi}_{h,i})_F = 0 \quad \forall \boldsymbol{\chi}_{h,i} \in V_{h,i}^F.$$

Since  $\nu_i|_F \in V_{h,i}^F$ , then (4.7) holds. A scaling argument similar to the one in [19, Lemma 5.1] shows that that  $\mathcal{Q}_{h,i}$  is stable and has optimal approximation properties in  $\|\cdot\|_{\Lambda_i}$ . We further note that the approximation property of the space  $V_{h,i}^{\Gamma}$  on  $\Gamma_i$ ,  $V_{h,i}^{\Gamma}|_F := V_{h,i}^F$ , does not affect the approximation property of  $\mathcal{Q}_{h,i}$ , but it affects the consistency error  $\mathcal{E}_c$ ; cf. Lemma 4.5.

Remark 4.1. The mortar condition A3 requires that the space  $\Lambda_h$  is controlled by the traces of the neighboring velocity spaces. We refer the reader to [19, section 7] for specific examples of  $V_h$  and  $\Lambda_h$  that satisfy A3.

We now have all the ingredients to set up problem (2.7) and therewith define the extension operator  $\mathcal{R}_{h,i}$ . In turn, the discrete spaces  $V_h \times W_h$  are defined as in (2.8). The discrete Stokes problem is then defined by (2.10), posed on  $V_h \times W_h$ , with the bilinear forms from (4.2). Equation (2.9b), which in this case is  $\sum_i ((\tilde{\mu}\varepsilon(\boldsymbol{u}_{h,i}), \varepsilon(\mathcal{R}_{h,i}\boldsymbol{\mu}_h))_{\Omega_i} - (\nabla \cdot \mathcal{R}_{h,i}\boldsymbol{\mu}_h, p_{h,i})_{\Omega_i} - (\boldsymbol{g}, \mathcal{R}_{h,i}\boldsymbol{\mu}_h)_{\Omega_i}) = 0 \ \forall \boldsymbol{\mu}_h \in \Lambda_h$ , imposes weakly continuity of normal stress.

**4.2.** Well-posedness. We next verify assumptions A1, A2, and A4 needed for the proofs of Theorems 2.1 and 2.2.

LEMMA 4.1 (A1). Problem (2.7) has a unique solution and the resulting extension operator  $\mathcal{R}_h: \Lambda \to V_h$  is continuous, i.e.,  $\|\mathcal{R}_h \boldsymbol{\lambda}\|_V \lesssim \|\boldsymbol{\lambda}\|_{\Lambda} \ \forall \boldsymbol{\lambda} \in \Lambda$ .

*Proof.* We first consider uniqueness by setting  $\lambda = 0$ . Setting  $w_{h,i} = 1$  in (2.7b) and using the divergence theorem and (2.7d), we obtain  $r_i = 0$ . Next, setting the test functions in (2.7a)–(2.7b) to  $(\mathcal{R}_{h,i}\lambda, p_{h,i}^{\lambda})$  and summing the equations gives us  $\mathcal{R}_{h,i}\lambda = 0$ , using Korn's inequality (4.5). Moreover, we have  $p_{h,i}^{\lambda} \perp S_{H,i}$  from (2.7c), so we use the inf-sup condition (4.6) and (2.7a) to derive that  $p_{h,i}^{\lambda} = 0$ .

It remains to show continuity. The first step is to obtain a bound on  $p_{h,i}^{\lambda}$ . Since  $p_{h,i}^{\lambda} \perp S_{H,i}$ , we use  $v_{h,i}^{0}$  from the inf-sup condition (4.6) as a test function and use the continuity of  $a_{i}(\cdot,\cdot)$  to obtain

$$\|\boldsymbol{v}_{h,i}^{0}\|_{V_{i}}\|p_{h,i}^{\lambda}\|_{W_{i}} \lesssim b_{i}\left(\boldsymbol{v}_{h,i}^{0}, p_{h,i}^{\lambda}\right) = a_{i}\left(\mathcal{R}_{h,i}\boldsymbol{\lambda}, \boldsymbol{v}_{h,i}^{0}\right) \lesssim \|\mathcal{R}_{h,i}\boldsymbol{\lambda}\|_{V_{i}}\|\boldsymbol{v}_{h,i}^{0}\|_{V_{i}}.$$

Thus,  $||p_{h,i}^{\lambda}||_{W_i} \lesssim ||\mathcal{R}_{h,i}\boldsymbol{\lambda}||_{V_i}$ .

Next, let  $\mathcal{R}_{h,i}^{\star} \lambda \in V_{h,i}$  be a continuous discrete extension operator [32, Theorem 4.1.3] satisfying  $\operatorname{Tr}_{i} \mathcal{R}_{h,i}^{\star} \lambda = \mathcal{Q}_{h,i} \lambda$  on  $\Gamma_{i}$  and

$$\|\mathcal{R}_{h,i}^{\star}\boldsymbol{\lambda}\|_{V_i} \lesssim \|\mathcal{Q}_{h,i}\boldsymbol{\lambda}\|_{\Lambda_i} \lesssim \|\boldsymbol{\lambda}\|_{\Lambda_i}.$$

We take as test functions in (2.7)  $\boldsymbol{v}_{h,i}^0 = \boldsymbol{\varphi}_{h,i}^0 := (\mathcal{R}_{h,i} - \mathcal{R}_{h,i}^{\star}) \boldsymbol{\lambda} \in V_{h,i}^0$ ,  $w_{h,i} = p_{h,i}^{\lambda}$ ,  $s_i = r_i$ , and combine the equations. Using Korn's inequality (4.5), the continuity of  $a_i$  and  $b_i$ , Young's inequality, and the bounds on  $p_{h,i}^{\lambda}$  and  $\mathcal{R}_{h,i}^{\star}\boldsymbol{\lambda}$ , we derive

$$\begin{aligned} \|\boldsymbol{\varphi}_{h,i}^{0}\|_{V_{i}}^{2} &\lesssim a_{i}\left(\boldsymbol{\varphi}_{h,i}^{0}, \boldsymbol{\varphi}_{h,i}^{0}\right) = -a_{i}\left(\mathcal{R}_{h,i}^{\star}\boldsymbol{\lambda}, \boldsymbol{\varphi}_{h,i}^{0}\right) + b_{i}\left(-\mathcal{R}_{h,i}^{\star}\boldsymbol{\lambda}, p_{h,i}^{\lambda}\right) \\ &\lesssim \|\mathcal{R}_{h,i}^{\star}\boldsymbol{\lambda}\|_{V_{i}}\left(\|\boldsymbol{\varphi}_{h,i}^{0}\|_{V_{i}} + \|p_{h,i}^{\lambda}\|_{W_{i}}\right) \lesssim \|\boldsymbol{\lambda}\|_{\Lambda_{i}}^{2} + \epsilon\left(\|\boldsymbol{\varphi}_{h,i}^{0}\|_{V_{i}}^{2} + \|\mathcal{R}_{h,i}\boldsymbol{\lambda}\|_{V_{i}}^{2}\right). \end{aligned}$$

Combining this bound with  $\|\mathcal{R}_{h,i}\boldsymbol{\lambda}\|_{V_i}^2 \lesssim \|\boldsymbol{\varphi}_{h,i}^0\|_{V_i}^2 + \|\mathcal{R}_{h,i}^{\star}\boldsymbol{\lambda}\|_{V_i}^2 \lesssim \|\boldsymbol{\varphi}_{h,i}^0\|_{V_i}^2 + \|\boldsymbol{\lambda}\|_{\Lambda_i}^2$  and taking  $\epsilon$  small enough, we obtain  $\|\boldsymbol{\varphi}_{h,i}^0\|_{V_i} \lesssim \|\boldsymbol{\lambda}\|_{\Lambda_i}$ , which implies  $\|\mathcal{R}_{h,i}\boldsymbol{\lambda}\|_{V_i} \lesssim \|\boldsymbol{\lambda}\|_{\Lambda_i}$  for  $i \in I_{\Omega}$ , concluding the proof.

LEMMA 4.2 (A2). The four inequalities (2.11) hold for  $V_h \times W_h$ .

*Proof.* First, the continuity of  $a_i$  and  $b_i$  from (4.2) follow from the Cauchy–Schwarz inequality. Summing over all  $i \in I_{\Omega}$  provides (2.11a)–(2.11b).

For (2.11c), the coercivity of  $a_i$ , Korn's inequality (4.4) cannot be applied locally, since the velocity is not restricted on subdomain boundaries. To that end, we recall that  $\Lambda_h = \text{Tr } \tilde{V}_h$ , where  $\tilde{V}_h \subset V$  is a conforming Lagrange finite element space on a mesh  $\tilde{\Omega}_h$  that is aligned with the domain decomposition. We can write  $\tilde{V}_{h,i}$ 

 $\tilde{V}_{h,i}^0 \oplus \mathcal{E}_{h,i}\Lambda_h$ , where  $\tilde{V}_{h,i}^0 = \{\tilde{v}_{h,i} \in \tilde{V}_{h,i} : \operatorname{Tr}_i \tilde{v}_{h,i} = 0 \text{ on } \Gamma_i\}$  and  $\mathcal{E}_{h,i} : \Lambda_h \to \tilde{V}_{h,i}$  is a discrete extension operator such that  $\mathcal{E}_{h,i}\mu_h = \mu_h$  on  $\Gamma_i$  and

$$(4.10) a_i \left( \mathcal{E}_{h,i} \boldsymbol{\mu}_h, \tilde{\boldsymbol{v}}_{h,i}^0 \right) = 0 \quad \forall \, \tilde{\boldsymbol{v}}_{h,i}^0 \in \tilde{V}_{h,i}^0.$$

Problem (4.10) is well-posed, since, due to (4.5),  $a_i(\cdot, \cdot)$  is coercive on  $\tilde{V}_{h,i}^0$ . Now, given  $\boldsymbol{u}_{h,i} = \boldsymbol{u}_{h,i}^0 + \mathcal{R}_{h,i}\boldsymbol{\lambda}_h$ , consider the local problem: Find  $\tilde{\boldsymbol{u}}_{h,i} = \tilde{\boldsymbol{u}}_{h,i}^0 + \mathcal{E}_{h,i}\boldsymbol{\lambda}_h \in \tilde{V}_{h,i}$  such that

$$(4.11) a_i \left( \tilde{\boldsymbol{u}}_{h,i}^0 + \mathcal{E}_{h,i} \boldsymbol{\lambda}_h, \tilde{\boldsymbol{v}}_{h,i}^0 + \mathcal{E}_{h,i} \boldsymbol{\lambda}_h \right) = a_i \left( \boldsymbol{u}_{h,i}, \tilde{\boldsymbol{v}}_{h,i}^0 + \mathcal{E}_{h,i} \boldsymbol{\lambda}_h \right) \forall \tilde{\boldsymbol{v}}_{h,i}^0 \in \tilde{V}_{h,i}^0.$$

Note that  $\boldsymbol{u}_{h,i}$  and  $\boldsymbol{\lambda}_h$  are given data. Problem (4.11) is well-posed, since, using (4.10),  $a_i(\tilde{\boldsymbol{u}}_{h,i}^0 + \mathcal{E}_{h,i}\boldsymbol{\lambda}_h, \tilde{\boldsymbol{v}}_{h,i}^0 + \mathcal{E}_{h,i}\boldsymbol{\lambda}_h) = a_i(\tilde{\boldsymbol{u}}_{h,i}^0, \tilde{\boldsymbol{v}}_{h,i}^0) + a_i(\mathcal{E}_{h,i}\boldsymbol{\lambda}_h, \mathcal{E}_{h,i}\boldsymbol{\lambda}_h)$ , and the coercivity follows from (4.5). We further note that (4.11) implies that  $a_i(\boldsymbol{u}_{h,i} - \tilde{\boldsymbol{u}}_{h,i}, \tilde{\boldsymbol{u}}_{h,i}) = 0$ . Also, (4.9) implies that,  $\forall \boldsymbol{m} \in \mathbf{RM}(\Omega_i)$ ,  $(\boldsymbol{u}_{h,i} - \tilde{\boldsymbol{u}}_{h,i}, \boldsymbol{m})_{\Gamma_i} = (\mathcal{Q}_{h,i}\boldsymbol{\lambda}_h - \boldsymbol{\lambda}_h, \boldsymbol{m})_{\Gamma_i} = 0$ . Hence, Korn's inequality (4.5) on  $\Omega_i$  gives  $\|\boldsymbol{u}_{h,i} - \tilde{\boldsymbol{u}}_{h,i}\|_{1,\Omega_i}^2 \lesssim a_i(\boldsymbol{u}_{h,i} - \tilde{\boldsymbol{u}}_{h,i}, \boldsymbol{u}_{h,i} - \tilde{\boldsymbol{u}}_{h,i})$ . Then, with  $\tilde{\boldsymbol{u}}_h \in \tilde{V}_h$  defined as  $\tilde{\boldsymbol{u}}_h|_{\Omega_i} = \tilde{\boldsymbol{u}}_{h,i}$ , we have

$$\sum_{i} a_{i}(\boldsymbol{u}_{h,i}, \boldsymbol{u}_{h,i}) = \sum_{i} a_{i}(\boldsymbol{u}_{h,i} - \tilde{\boldsymbol{u}}_{h,i}, \boldsymbol{u}_{h,i} - \tilde{\boldsymbol{u}}_{h,i}) + \sum_{i} a_{i}(\tilde{\boldsymbol{u}}_{h,i}, \tilde{\boldsymbol{u}}_{h,i})$$

$$\gtrsim \sum_{i} \|\boldsymbol{u}_{h,i} - \tilde{\boldsymbol{u}}_{h,i}\|_{1,\Omega_{i}}^{2} + \|\tilde{\boldsymbol{u}}_{h}\|_{1,\Omega}^{2} \gtrsim \sum_{i} \|\boldsymbol{u}_{h,i}\|_{1,\Omega_{i}}^{2},$$

where in the first inequality we used Korn's inequality (4.5) applied globally on  $\Omega$ . This completes the proof of (2.11c).

Next, we prove the inf-sup condition (2.11d) by constructing  $\mathbf{v}_h \in V_h$  for a given  $w_h \in W_h$ . As in Lemma 3.4, we consider a global divergence problem on  $\Omega$  (cf. (3.17)) to construct  $\mathbf{v}^w \in (H^1(\Omega))^n$  with the properties

$$\nabla \cdot \boldsymbol{v}^w = w_h \text{ in } \Omega, \quad \boldsymbol{v}^w = 0 \text{ on } \partial_u \Omega, \quad \|\boldsymbol{v}^w\|_{1,\Omega} \lesssim \|w_h\|_{\Omega}.$$

The approach used in Lemma 3.4 to construct  $\boldsymbol{\mu}_h \in \Lambda_h$  does not work here, due to the global continuity of  $\Lambda_h$ . Instead, we consider a discrete Stokes problem in  $\Omega$  based on the finite element pair  $\tilde{V}_h \times W_H$ , where we recall that  $\Lambda_h = \operatorname{Tr} \tilde{V}_h$  and we define  $W_H$  to be the space of piecewise constants on the partition formed by the subdomains  $\Omega_i$ . Assuming that there is at least one interior vertex in each  $\Gamma_{ij}$ , the pair  $\tilde{V}_h \times W_H$  is inf-sup stable; see [35, Lemma 3.3]. Let  $\tilde{\boldsymbol{u}}_h^w \in \tilde{V}_h$  be a discrete Stokes projection of  $\boldsymbol{v}^w$  in  $\Omega$  based on solving the problem, Find  $(\tilde{\boldsymbol{u}}_h^w, p_H^w) \in \tilde{V}_h \times W_H$  such that

(4.12a) 
$$(\nabla \tilde{\boldsymbol{u}}_{h}^{w}, \nabla \tilde{\boldsymbol{v}}_{h})_{\Omega} - (\nabla \cdot \tilde{\boldsymbol{v}}_{h}, p_{H}^{w})_{\Omega} = (\nabla \boldsymbol{v}^{w}, \nabla \tilde{\boldsymbol{v}}_{h})_{\Omega} \qquad \forall \tilde{\boldsymbol{v}}_{h} \in \tilde{V}_{h},$$
(4.12b) 
$$(\nabla \cdot \tilde{\boldsymbol{u}}_{h}^{w}, w_{H})_{\Omega} = (\nabla \cdot \boldsymbol{v}^{w}, w_{H})_{\Omega} \qquad \forall w_{H} \in W_{H}.$$

The continuity of the Stokes finite element approximation implies  $\|\tilde{\boldsymbol{u}}_h^w\|_{1,\Omega} \lesssim \|\boldsymbol{v}^w\|_{1,\Omega}$ . We now define  $\boldsymbol{\mu}_h := \operatorname{Tr} \tilde{\boldsymbol{u}}_h^w \in \Lambda_h$ . The trace inequality implies

$$\sum_{i} \|\boldsymbol{\mu}_{h}\|_{\Lambda_{i}} \lesssim \sum_{i} \|\tilde{\boldsymbol{u}}_{h}^{w}\|_{1,\Omega_{i}} \lesssim \|\boldsymbol{v}^{w}\|_{1,\Omega} \lesssim \|w_{h}\|_{\Omega}.$$

Moreover, (4.12b) gives

$$(\boldsymbol{\nu}_i \cdot \boldsymbol{\mu}_h, 1)_{\Gamma_i} = (\nabla \cdot \tilde{\boldsymbol{u}}_h^w, 1)_{\Omega_i} = (\nabla \cdot \boldsymbol{v}^w, 1)_{\Omega_i} = (w_h, 1)_{\Omega_i}.$$

Now, using (2.7d) and (4.7), we obtain

$$(\nabla \cdot \mathcal{R}_{h,i}\boldsymbol{\mu}_h, 1)_{\Omega_i} = (\boldsymbol{\nu}_i \cdot \mathcal{Q}_{h,i}\boldsymbol{\mu}_h, 1)_{\Gamma_i} = (\boldsymbol{\nu}_i \cdot \boldsymbol{\mu}_h, 1)_{\Gamma_i} = (w_h, 1)_{\Omega_i}.$$

Using the discrete inf-sup condition (4.6), we construct  $v_{h,i}^0 \in V_{h,i}^0$  such that

$$\nabla \cdot \boldsymbol{v}_{h,i}^0 = w_{h,i} - \nabla \cdot \mathcal{R}_{h,i} \boldsymbol{\mu}_h \text{ in } \Omega_i, \quad \|\boldsymbol{v}_{h,i}^0\|_{1,\Omega_i} \lesssim \|w_{h,i} - \nabla \cdot \mathcal{R}_{h,i} \boldsymbol{\mu}_h\|_{\Omega_i},$$

and set  $\mathbf{v}_{h,i} = \mathbf{v}_{h,i}^0 + \mathcal{R}_{h,i} \boldsymbol{\mu}_h$ . We have

(4.13a) 
$$\sum_{i} b_{i}(\boldsymbol{v}_{h,i}, w_{h,i}) = \|w_{h}\|_{\Omega}^{2},$$

(4.13b) 
$$\sum_{i} \|\mathbf{v}_{h,i}\|_{V_{i}} \lesssim \sum_{i} \|\mathcal{R}_{h,i}\boldsymbol{\mu}_{h}\|_{V_{i}} + \|\mathbf{w}_{h}\|_{\Omega} \lesssim \|\mathbf{w}_{h}\|_{W},$$

using Lemma 4.1 in the last inequality. This implies the inf-sup condition (2.11d).  $\Box$ 

LEMMA 4.3 (A4). For each subdomain  $\Omega_i$ , it holds that

$$\|\boldsymbol{v}_{h,i}\|_{\Gamma_i} \lesssim \|\boldsymbol{v}_{h,i}\|_{V_i} \quad \forall \boldsymbol{v}_{h,i} \in V_{h,i}.$$

*Proof.* The statement follows from the trace inequality  $\|\mathbf{v}_i\|_{\frac{1}{2},\Gamma_i} \lesssim \|\mathbf{v}_i\|_{1,\Omega_i}$ .

**4.3. Interpolation operators.** We next define appropriate interpolants in the discrete spaces. We define  $\Pi^W$  as the  $L^2$ -projection onto  $W_h$ ,  $\Pi^{\Lambda}$  as the  $L^2$ -projection onto  $\Lambda_h$ , and  $\Pi_i^{V^{\Gamma}}$  as the  $L^2$ -projection onto  $V_{h,i}^{\Gamma}$ .

For the interpolant  $\Pi^V$ , we note that the construction from section 3.3 uses  $\operatorname{Tr}_i\Pi_i^V=\mathcal{Q}_{h,i}\operatorname{Tr}_i$  on  $\Gamma_i$ . However, canonical b-compatible interpolants for Stokes finite elements do not typically satisfy this property. For this reason, we define  $\Pi_i^V$  as a suitable Stokes elliptic projection. More precisely, for  $i\in I_{\Omega}$ , given  $\boldsymbol{u}_i$ , we consider the discrete Stokes problem: Find  $(\Pi_i^V\boldsymbol{u}_i,p_{h,i}^u)\in V_{h,i}\times W_{h,i}^0$  such that

$$(4.15a) \quad \left(\nabla(\Pi_i^V \boldsymbol{u}_i), \nabla \boldsymbol{v}_{h,i}^0\right)_{\Omega_i} - \left(\nabla \cdot \boldsymbol{v}_{h,i}^0, p_{h,i}^u\right)_{\Omega_i} = \left(\nabla \boldsymbol{u}_i, \nabla \boldsymbol{v}_{h,i}^0\right)_{\Omega_i} \quad \forall \boldsymbol{v}_{h,i}^0 \in V_{h,i}^0,$$

$$(4.15b) \qquad (\nabla \cdot \prod_{i}^{V} \boldsymbol{u}_{i}, w_{h,i})_{\Omega_{i}} = (\nabla \cdot \boldsymbol{u}_{i}, w_{h,i})_{\Omega_{i}} \quad \forall w_{h,i} \in W_{h,i},$$

(4.15c) 
$$\operatorname{Tr}_{i} \Pi_{i}^{V} \boldsymbol{u}_{i} = \mathcal{Q}_{h,i} \operatorname{Tr}_{i} \boldsymbol{u}_{i} \quad \text{on } \Gamma_{i}.$$

The well-posedness of the above problem and optimal approximation properties of  $\Pi_i^V$  follow from standard Stokes finite element analysis [9].

Let  $\lambda = \text{Tr } \boldsymbol{u}$ . Note that, by construction, we have  $\text{Tr}_i \Pi_i^V = \mathcal{Q}_{h,i} \text{Tr}_i$  on  $\Gamma_i$ . Therefore  $\Pi_i^V(\boldsymbol{u}_i - \mathcal{R}_{h,i}\lambda) \in V_{h,i}^0$ . Using this observation, the interpolant  $\Pi^V$  onto  $V_h$  is defined similarly to (3.24a):

$$(4.16) \qquad \Pi^{V} \boldsymbol{u} := \mathcal{R}_{h} \Pi^{\Lambda} \lambda + \bigoplus_{i} \Pi_{i}^{V} (\boldsymbol{u}_{i} - \mathcal{R}_{h,i} \lambda) = \mathcal{R}_{h} (\Pi^{\Lambda} \lambda - \lambda) + \bigoplus_{i} \Pi_{i}^{V} \boldsymbol{u}_{i}.$$

The continuity of  $\mathcal{R}_h$ , established in Lemma 4.1, implies the following approximation property of  $\Pi^V$ :

Lemma 4.4 (A5). The interpolation operator  $\Pi^V$  has the property

$$(4.18) b(\boldsymbol{u} - \Pi^{V} \boldsymbol{u}, w_h) = 0 \quad \forall w_h \in W_h.$$

*Proof.* We first note that b-compatibility of  $\Pi_i^V$  is ensured by (4.15b). The arguments from Lemma 3.7 now provide the result.

## 4.4. Consistency error.

Lemma 4.5. Given A3, then the consistency error  $\mathcal{E}_c$  satisfies

$$\mathcal{E}_c \lesssim \sum_i \|\Pi_i^{V^{\Gamma}}(\sigma oldsymbol{
u}) - \sigma oldsymbol{
u}\|_{\Gamma_i}.$$

*Proof.* We consider the term in the numerator of the definition (2.15) of  $\mathcal{E}_c$ . We recall the definitions of the bilinear forms in (4.2) and apply integration by parts. Given  $(\boldsymbol{u}, p)$  the solution to (4.1), we substitute the momentum balance (4.1b) and the boundary conditions (4.1c) to derive

$$\sum_{i} (a_i(\boldsymbol{u}, \boldsymbol{v}_h) - b_i(\boldsymbol{v}_h, p) - (\boldsymbol{g}, \boldsymbol{v}_h)_{\Omega_i}) = \sum_{i} (\sigma \boldsymbol{\nu}_i, \boldsymbol{v}_{h,i})_{\partial \Omega_i} = \sum_{i} (\sigma \boldsymbol{\nu}_i, \boldsymbol{v}_{h,i})_{\Gamma_i}.$$

We proceed as in section 3.4.2. Let  $\mathbf{v}_{h,i} = \mathbf{v}_{h,i}^0 + \mathcal{R}_{h,i} \boldsymbol{\mu}_h$ . Using the continuity of  $\sigma$  on  $\Gamma$  and assumption A3, we obtain

$$\begin{split} \sum_{i} (\sigma \boldsymbol{\nu}_{i}, \boldsymbol{v}_{h,i})_{\Gamma_{i}} &= \sum_{i} (\sigma \boldsymbol{\nu}_{i}, \mathcal{Q}_{h,i} \boldsymbol{\mu}_{h})_{\Gamma_{i}} \\ &= \sum_{i} \left( \left( \sigma \boldsymbol{\nu}_{i} - \boldsymbol{\Pi}_{i}^{V^{\Gamma}} (\sigma \boldsymbol{\nu}_{i}), \mathcal{Q}_{h,i} \boldsymbol{\mu}_{h} \right)_{\Gamma_{i}} + (\boldsymbol{\Pi}_{i}^{V^{\Gamma}} (\sigma \boldsymbol{\nu}_{i}), \boldsymbol{\mu}_{h})_{\Gamma_{i}} \right) \\ &= \sum_{i} \left( \left( \sigma \boldsymbol{\nu}_{i} - \boldsymbol{\Pi}_{i}^{V^{\Gamma}} (\sigma \boldsymbol{\nu}_{i}), \mathcal{Q}_{h,i} \boldsymbol{\mu}_{h} \right)_{\Gamma_{i}} + (\boldsymbol{\Pi}_{i}^{V^{\Gamma}} (\sigma \boldsymbol{\nu}_{i}) - \sigma \boldsymbol{\nu}_{i}, \boldsymbol{\mu}_{h})_{\Gamma_{i}} \right) \\ &\lesssim \sum_{i} \|\sigma \boldsymbol{\nu}_{i} - \boldsymbol{\Pi}_{i}^{V^{\Gamma}} (\sigma \boldsymbol{\nu}_{i})\|_{\Gamma_{i}} \|\mathcal{Q}_{h,i} \boldsymbol{\mu}_{h}\|_{\Gamma_{i}} \\ &= \sum_{i} \|\sigma \boldsymbol{\nu}_{i} - \boldsymbol{\Pi}_{i}^{V^{\Gamma}} (\sigma \boldsymbol{\nu}_{i})\|_{\Gamma_{i}} \|\boldsymbol{v}_{h,i}\|_{\Gamma_{i}} \\ &\lesssim \sum_{i} \|\sigma \boldsymbol{\nu}_{i} - \boldsymbol{\Pi}_{i}^{V^{\Gamma}} (\sigma \boldsymbol{\nu}_{i})\|_{\Gamma_{i}} \|\boldsymbol{v}_{h,i}\|_{1,\Omega_{i}}, \end{split}$$

using the trace inequality,  $\forall i \in I_{\Omega}$ ,  $\|\boldsymbol{v}_{h,i}\|_{\Gamma_i} \lesssim \|\boldsymbol{v}_{h,i}\|_{\Lambda_i} \lesssim \|\boldsymbol{v}_{h,i}\|_{1,\Omega_i}$ .

**4.5. Main result.** We conclude this section with its main result, which follows directly from Lemmas 4.1–4.5 combined with Theorems 2.1–2.3.

THEOREM 4.6. The flux-mortar mixed finite element method for the Stokes problem given by (2.10) with (4.2) admits a unique solution  $(\mathbf{u}_h, p_h) \in V_h \times W_h$  that satisfies

$$\|\boldsymbol{u}_h\|_V + \|p_h\|_W \lesssim \sum_i \|\boldsymbol{g}_i\|_{-1,\Omega_i} + \|f\|_{\Omega}.$$

Furthermore, if A3 holds, then the mortar solution  $\lambda_h \in \Lambda_h$  is unique and the error with respect to the true solution  $(\boldsymbol{u}, p)$  satisfies

$$\|\boldsymbol{u} - \boldsymbol{u}_h\|_V + \|p - p_h\|_W \lesssim \|\Pi^V \boldsymbol{u} - \boldsymbol{u}\|_V + \|\Pi^W p - p\|_W + \sum_i \|\Pi_i^{V^{\Gamma}}(\sigma \boldsymbol{\nu}) - \sigma \boldsymbol{\nu}\|_{\Gamma_i}.$$

Remark 4.2. A bound on the mortar error  $\|\lambda - \lambda_h\|_{\Lambda}$  can be derived using an argument similar to the proof of Theorem 3.11, under the stronger mortar condition  $\|\mu_h\|_{\Lambda_i} \lesssim \|\mathcal{Q}_{h,i}\mu_h\|_{\Lambda_i} \,\forall \, \mu_h \in \Lambda_h$ . Examples for the latter are given in [19, section 7].

**4.6.** Interface problem. We end this section by reducing the Stokes flow problem to a flux-mortar interface problem following the four steps (2.23)–(2.26) from section 2.5. To accommodate its construction, we require A6, presented in the following lemma.

LEMMA 4.7 (A6). The following inf-sup condition holds for the spaces  $\Lambda_h \times S_H$ :

$$\forall s_H \in S_H, \exists 0 \neq \boldsymbol{\mu}_h \in \Lambda_h \text{ such that } b(\mathcal{R}_h \boldsymbol{\mu}_h, s_H) \gtrsim \|\boldsymbol{\mu}_h\|_{\Lambda} \|s_H\|_W.$$

*Proof.* Setting  $w_h := s_H \in S_H \subseteq W_h$  in the proof of the inf-sup condition (2.11d) in Lemma 4.2 leads to a pair  $(\boldsymbol{v}_h^0, \boldsymbol{\mu}_h)$  with  $\boldsymbol{v}_h^0 = 0$  that satisfies (4.13).

5. Numerical results. In this section, we return to the model problem describing porous medium flow and test the theoretical results from section 3.4 with the use of numerical experiments. The numerical code, implemented in DuMu<sup>X</sup> [15, 25], is available for download at git.iws.uni-stuttgart.de/dumux-pub/boon2019a. The lowest order Raviart-Thomas mixed finite element method reduced to a finite volume scheme with a two-point flux approximation is applied in each subdomain and we solve the problem using the iterative scheme described in section 2.5. On the mortar grids, we investigate two options, namely the use of piecewise constant functions ( $\mathcal{P}_0$ ) and linear Lagrange basis functions ( $\mathcal{P}_1$ ). Moreover, both the projection operators  $\mathcal{Q}_h^{\flat}$  are considered in order to cover all results from section 3.4.

The setup of the test is as follows. Let the domain  $\Omega = (0,1) \times (0,2)$ , the permeability K = 1, and the pressure and velocity be given by

(5.1a) 
$$p(x,y) = y^2 \left(1 - \frac{y}{3}\right) + x(1-x)y\sin(2\pi x),$$

(5.1b) 
$$\mathbf{u}(x,y) = -\begin{bmatrix} y((1-2x)\sin(2\pi x) - 2\pi(x-1)x\cos(2\pi x)) \\ (2-y)y + x(1-x)\sin(2\pi x) \end{bmatrix}.$$

We prescribe the pressure on the boundary  $\partial\Omega$  and define the source function  $f:=\nabla\cdot \boldsymbol{u}$  to match with these chosen distributions.

We partition the domain into four subdomains by introducing interfaces along the lines x=0.5 and y=1. In order to investigate the convergence rates from section 3.4, we test a sequence of refinements by a factor two. Each subdomain is meshed with a rectangular grid such that the meshes are nonmatching at each of the four interfaces. The meshes on the coarsest level are  $5 \times 9$  on  $(0,0.5) \times (0,1)$ ,  $5 \times 13$  on  $(0.5,1) \times (0,1)$ ,  $7 \times 13$  on  $(0,0.5) \times (1,2)$ , and  $7 \times 9$  on  $(0.5,1) \times (1,2)$ . The mortar grids are generated such that each interface has the same number of elements. We refer to the number of mortar grid elements per interface on the coarsest level as  $n_{\Gamma}^0$  and we consider the two cases  $n_{\Gamma}^0 \in \{2,3\}$ . For an illustration of the grid and the solution  $(\boldsymbol{u}_h, p_h)$ , we refer to Figure 1.

We analyze the decrease of the errors of the velocity  $e_u := \|\boldsymbol{u} - \boldsymbol{u}_h\|_{\Omega}$  and  $e_{div(u)} := \sum_i \|\nabla \cdot (\boldsymbol{u} - \boldsymbol{u}_h)\|_{\Omega_i}$ , the pressure  $e_p := \|p - p_h\|_{\Omega}$ , the flux-mortar  $e_{\lambda} := \|\lambda - \lambda_h\|_{\Gamma}$ , and the projected flux-mortar  $e_{Q\lambda} := \|\lambda - Q_h\lambda_h\|_{\Gamma}$ . Convergence results for  $n_{\Gamma}^0 = 2$  are presented in Tables 1 and 2 for  $\mathcal{P}_1$  and  $\mathcal{P}_0$  mortars, respectively. The mortar grid is sufficiently coarse to fulfill the mortar condition A3 for both  $\mathcal{Q}_h^{\flat}$  and  $\mathcal{Q}_h^{\sharp}$ . The rates  $r_u$  and  $r_p$  from Table 1 indicate first order convergence for the velocity and pressure for both projectors  $\mathcal{Q}_h^{\flat}$  and  $\mathcal{Q}_h^{\sharp}$  in the case of  $\mathcal{P}_1$  mortars. Table 2 shows that the choice of  $\mathcal{P}_0$  mortars results in a reduction for the velocity with the rate approaching  $O(h^{1/2})$ . We note that Theorems 3.9 and 3.10 predict O(h) convergence for  $\mathcal{Q}_h^{\sharp}$  with

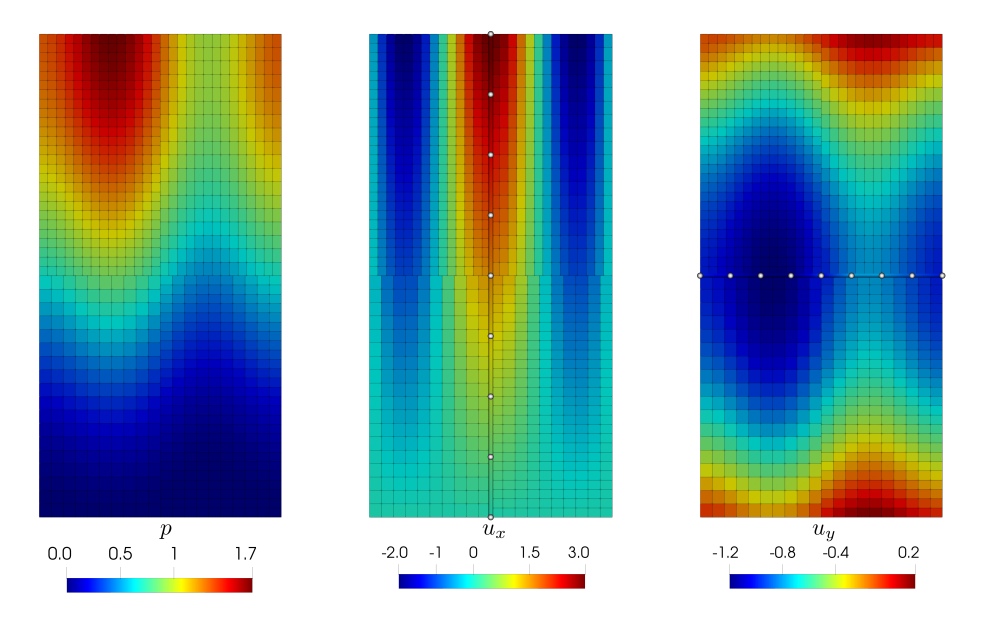


FIG. 1. Pressure (left) and velocity (center and right) distributions computed after the first refinement using continuous, piecewise linear mortars  $(\mathcal{P}_1)$ , and initial mortar grid with  $n_{\Gamma}^0=2$ . The vertical (center) and horizontal (right) mortar grids are visualized as tubes with white circles indicating the vertices.

Table 1 Errors and convergence rates for  $n_{\Gamma}^0=2$  and  $\mathcal{P}_1$  mortans.

$\mathcal{P}_1$	$  e_u^{\flat}$	$r_u^{\flat}$	$e_{div(u)}^{\flat}$	$r_{div(u)}^{\flat}$	$  e_p^{\flat}$	$r_p^{\flat}$	$\mid e_{\lambda}^{\flat} \mid$	$r_\lambda^{\flat}$	$e_{\mathcal{Q}\lambda}^{\flat}$	$r_{\mathcal{Q}\lambda}^{\flat}$
0	7.05e-2		2.78e+0		4.43e-2		3.78e-2		1.05e-1	
1	2.76e-2	1.35	1.39e + 0	1.00	2.18e-2	1.02	1.78e-2	1.08	5.22e-2	1.01
2	1.26e-2	1.14	6.96e-1	1.00	1.08e-2	1.01	1.13e-2	0.65	2.79e-2	0.91
3	6.11e-3	1.04	3.48e-1	1.00	5.42e-3	1.00	7.91e-3	0.52	1.59e-2	0.81
4	3.03e-3	1.01	1.74e-1	1.00	2.71e-3	1.00	5.58e-3	0.50	9.62e-3	0.72
5	1.51e-3	1.00	8.70e-2	1.00	1.35e-3	1.00	3.95e-3	0.50	6.15e-3	0.64
6	7.56e-4	1.00	4.35e-2	1.00	6.77e-4	1.00	2.79e-3	0.50	4.10e-3	0.58
7	3.78e-4	1.00	2.17e-2	1.00	3.38e-4	1.00	1.97e-3	0.50	2.81e-3	0.55
	$e_u^{\sharp}$	$r_u^{\sharp}$	$e_{div(u)}^{\sharp}$	$r_{div(u)}^{\sharp}$	$e_p^{\sharp}$	$r_p^{\sharp}$	$  e_{\lambda}^{\sharp}  $	$r_\lambda^\sharp$	$\left  \begin{array}{c} e_{\mathcal{Q}\lambda}^{\sharp} \end{array} \right $	$r_{\mathcal{Q}\lambda}^{\sharp}$
0	7.05e-2		2.78e + 0		4.43e-2		3.78e-2		1.05e-1	
1	2.76e-2	1.35	1.39e + 0	1.00	2.18e-2	1.02	1.79e-2	1.08	5.23e-2	1.01
2	1.26e-2	1.14	6.96e-1	1.00	1.08e-2	1.01	1.14e-2	0.65	2.79e-2	0.91
3	6.11e-3	1.04	3.48e-1	1.00	5.42e-3	1.00	7.92e-3	0.52	1.59e-2	0.81
4	3.03e-3	1.01	1.74e-1	1.00	2.71e-3	1.00	5.59e-3	0.50	9.62e-3	0.72
5	1.51e-3	1.00	8.70e-2	1.00	1.35e-3	1.00	3.95e-3	0.50	6.16e-3	0.64
6	7.56e-4	1.00	4.35e-2	1.00	6.77e-4	1.00	2.79e-3	0.50	4.11e-3	0.58
7	3.78e-4	1.00	2.17e-2	1.00	3.38e-4	1.00	1.98e-3	0.50	2.81e-3	0.55

 $\mathcal{P}_1$  mortars, while  $O(h^{1/2})$  is predicted in the other cases. For the mortar variable, the rates  $r_{\lambda}$  and  $r_{\mathcal{Q}\lambda}$  are lower by approximately one half compared to  $r_u$  and  $r_p$ . This is in agreement with Theorem 3.11. Finally, we note that the error  $e_{div(u)}$  is identical and first order convergent in all cases, which is consistent with (3.29).

The most striking observation in both of these tables is that the two extension operators  $\mathcal{R}_h^{\flat}$  and  $\mathcal{R}_h^{\sharp}$  produce nearly indistinguishable solutions. However, we have

Table 2 Errors and convergence rates for  $n_{\Gamma}^0=2$  and  $\mathcal{P}_0$  mortans.

$\mathcal{P}_0$	$e_u^{\flat}$	$r_u^{\flat}$	$e_{div(u)}^{\flat}$	$r_{div(u)}^{\flat}$	$e_p^{\flat}$	$r_p^{\flat}$	$\mid e_{\lambda}^{\flat} \mid$	$r_\lambda^{\flat}$	$e_{\mathcal{Q}\lambda}^{\flat}$	$r_{\mathcal{Q}\lambda}^{\flat}$
0	1.37e-1		2.78e+0		4.48e-2		3.41e-1		4.20e-1	
1	4.78e-2	1.51	1.39e+0	1.00	2.18e-2	1.04	1.70e-1	1.01	2.06e-1	1.03
2	1.85e-2	1.37	6.96e-1	1.00	1.08e-2	1.01	8.56e-2	0.99	1.03e-1	0.99
3	7.91e-3	1.23	3.48e-1	1.00	5.42e-3	1.00	4.49e-2	0.93	5.41e-2	0.93
4	3.72e-3	1.09	1.74e-1	1.00	2.71e-3	1.00	2.62e-2	0.77	3.18e-2	0.76
5	1.92e-3	0.96	8.70e-2	1.00	1.35e-3	1.00	1.88e-2	0.48	2.33e-2	0.45
6	1.07e-3	0.83	4.35e-2	1.00	6.77e-4	1.00	1.64e-2	0.20	2.08e-2	0.17
7	6.50e-4	0.72	2.17e-2	1.00	3.38e-4	1.00	1.57e-2	0.06	2.01e-2	0.05
	$e_u^{\sharp}$	$r_u^{\sharp}$	$e_{div(u)}^{\sharp}$	$r_{div(u)}^{\sharp}$	$e_p^{\sharp}$	$r_p^{\sharp}$	$e^{\sharp}_{\lambda}$	$r^{\sharp}_{\lambda}$	$e_{Q\lambda}^{\sharp}$	$r_{\mathcal{Q}\lambda}^{\sharp}$
0	$\begin{array}{ c c } \hline & e_u^{\sharp} \\ \hline & 1.37\text{e-}1 \end{array}$	$r_u^{\sharp}$	$\begin{array}{ c c } e_{div(u)}^{\sharp} \\ \hline 2.78e+0 \end{array}$	$r_{div(u)}^{\sharp}$	$e_p^{\sharp}$ $4.48e-2$	$r_p^{\sharp}$	$e_{\lambda}^{\sharp}$ 3.41e-1	$r^{\sharp}_{\lambda}$	$e_{\mathcal{Q}\lambda}^{\sharp}$ $4.19e-1$	$r_{\mathcal{Q}\lambda}^{\sharp}$
0	1	$r_u^{\sharp}$ 1.52		$r_{div(u)}^{\sharp}$ $1.00$		$r_p^{\sharp}$ 1.04		$r_{\lambda}^{\sharp}$ 1.01		$r_{\mathcal{Q}\lambda}^{\sharp}$ $1.03$
	1.37e-1		2.78e+0		4.48e-2		3.41e-1		4.19e-1	
1	1.37e-1 4.78e-2	1.52	2.78e+0 1.39e+0	1.00	4.48e-2 2.18e-2	1.04	3.41e-1 1.70e-1	1.01	4.19e-1 2.05e-1	1.03
$\frac{1}{2}$	1.37e-1 4.78e-2 1.85e-2	1.52 1.37	2.78e+0 1.39e+0 6.96e-1	1.00 1.00	4.48e-2 2.18e-2 1.08e-2	1.04 1.01	3.41e-1 1.70e-1 8.56e-2	1.01 0.99	4.19e-1 2.05e-1 1.03e-1	1.03 0.99
1 2 3	1.37e-1 4.78e-2 1.85e-2 7.91e-3	1.52 1.37 1.23	2.78e+0 1.39e+0 6.96e-1 3.48e-1	1.00 1.00 1.00	4.48e-2   2.18e-2   1.08e-2   5.42e-3	1.04 1.01 1.00	3.41e-1 1.70e-1 8.56e-2 4.49e-2	1.01 0.99 0.93	4.19e-1 2.05e-1 1.03e-1 5.40e-2	1.03 0.99 0.93
1 2 3 4	1.37e-1 4.78e-2 1.85e-2 7.91e-3 3.72e-3	1.52 1.37 1.23 1.09	2.78e+0 1.39e+0 6.96e-1 3.48e-1 1.74e-1	1.00 1.00 1.00 1.00	4.48e-2   2.18e-2   1.08e-2   5.42e-3   2.71e-3	1.04 1.01 1.00 1.00	3.41e-1 1.70e-1 8.56e-2 4.49e-2 2.62e-2	1.01 0.99 0.93 0.77	4.19e-1 2.05e-1 1.03e-1 5.40e-2 3.18e-2	1.03 0.99 0.93 0.76

Table 3 Errors and convergence rates for  $n_{\Gamma}^0=3$  and  $\mathcal{P}_1$  mortans.

	$\mid e_u^{\flat} \mid$	$r_u^{\flat}$	$e_{div(u)}^{\flat}$	$r_{div(u)}^{\flat}$	$e_p^{\flat}$	$r_p^{\flat}$	$\mid e_{\lambda}^{\flat} \mid$	$r_\lambda^{\flat}$	$e_{\mathcal{Q}\lambda}^{\flat}$	$r_{\mathcal{Q}\lambda}^{\flat}$
0	7.08e-2		2.78e+0		4.43e-2		4.51e-2		1.10e-1	
1	2.82e-2	1.33	1.39e + 0	1.00	2.18e-2	1.02	3.37e-2	0.42	6.37e-2	0.79
2	1.29e-2	1.13	6.96e-1	1.00	1.08e-2	1.01	2.41e-2	0.48	3.90e-2	0.71
3	6.31e-3	1.03	3.48e-1	1.00	5.42e-3	1.00	1.74e-2	0.47	2.55e-2	0.61
4	3.15e-3	1.00	1.74e-1	1.00	2.71e-3	1.00	1.29e-2	0.43	1.78e-2	0.52
5	1.60e-3	0.98	8.70e-2	1.00	1.35e-3	1.00	9.91e-3	0.38	1.34e-2	0.42
6	8.19e-4	0.96	4.35e-2	1.00	6.77e-4	1.00	8.03e-3	0.30	1.07e-2	0.32
7	4.30e-4	0.93	2.17e-2	1.00	3.38e-4	1.00	6.91e-3	0.22	9.21e-3	0.22

verified numerically that  $\mathcal{R}_h^{\flat}$  does not produce velocity fields with weakly continuous fluxes across the interfaces, so it is indeed different from  $\mathcal{R}_h^{\sharp}$ . The closeness of the results indicates that the interface consistency error  $\mathcal{E}_c$  is dominated by the subdomain discretization error. It may also be possible to improve the consistency error bound (3.33) for  $\mathcal{R}_h^{\flat}$  and make it comparable to the bound (3.32) for  $\mathcal{R}_h^{\sharp}$ .

We next consider the case of finer mortar grids with  $n_{\Gamma}^0 = 3$ , focusing on  $\mathcal{P}_1$  mortars. In Table 3, we show the errors and convergence rates with the projection operator  $\mathcal{Q}_h^b$ , noting that the results with  $\mathcal{Q}_h^b$  are similar. We observe a deterioration in the rates  $r_u$ ,  $r_{\lambda}$ , and  $r_{\mathcal{Q}\lambda}$ , compared to the case with  $n_{\Gamma}^0 = 2$ ; cf. Table 1. To illustrate this effect, we show in Figure 2 the mortar solution  $\lambda_h$  obtained on refinement level 5 with the coarser mortar grid  $n_{\Gamma}^0 = 2$  and the finer mortar grid  $n_{\Gamma}^0 = 3$ . We first note that in both cases an oscillation appears at the junction of the two mortar grids. It is likely due to the Gibbs phenomenon at the end points of the interfaces, in combination with the effect of the nonmatching grids. This oscillation is localized and it does not affect the global accuracy. However, in the finer mortar grid case, an oscillation is also observed along the entire interface. This indicates that the mortar condition A3 may be violated in this case.

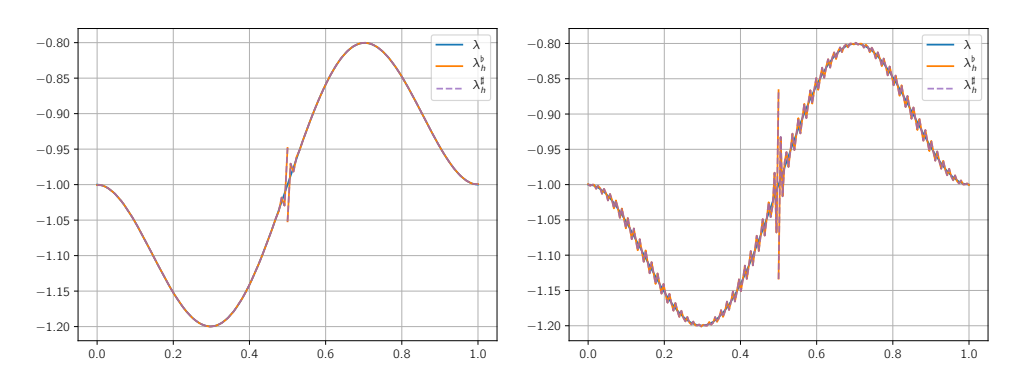


Fig. 2. Plot of the true flux  $\lambda$  and the discrete mortar solution  $\lambda_h$  along the line y=1, on refinement level 5 with initial mortar grid  $n_{\Gamma}^0=2$  (left) and  $n_{\Gamma}^0=3$  (right).

6. Conclusions. We have proposed a mortar method for a wide class of saddle point problems in which the continuity of the essential boundary condition variable, which is typically flux in flow or stress in elasticity, is enforced strongly using an interface variable. The method is capable of handling nonmatching grids under the mortar assumption A3. The method was presented and analyzed in an abstract setting. Specific examples concerning Darcy flow, Stokes flow, and Stokes–Darcy flow were shown to fit the framework. Numerical examples for Darcy flow were presented, verifying the theoretical convergence rates. It was further observed that violating A3 may result in spurious oscillations and reduced convergence in the mortar flux.

## REFERENCES

- R. Araya, C. Harder, D. Paredes, and F. Valentin, Multiscale hybrid-mixed method, SIAM J. Numer. Anal., 51 (2013), pp. 3505–3531, https://doi.org/10.1137/120888223.
- [2] R. Araya, C. Harder, A. H. Poza, and F. Valentin, Multiscale hybrid-mixed method for the Stokes and Brinkman equations-the method, Comput. Methods Appl. Mech. Engrg., 324 (2017), pp. 29–53.
- T. Arbogast, Analysis of a two-scale, locally conservative subgrid upscaling for elliptic problems, SIAM J. Numer. Anal., 42 (2004), pp. 576-598, https://doi.org/10.1137/ S0036142902406636.
- [4] T. Arbogast, L. C. Cowsar, M. F. Wheeler, and I. Yotov, Mixed finite element methods on nonmatching multiblock grids, SIAM J. Numer. Anal., 37 (2000), pp. 1295–1315, https://doi.org/10.1137/S0036142996308447.
- [5] T. Arbogast, G. Pencheva, M. F. Wheeler, and I. Yotov, A multiscale mortar mixed finite element method, Multiscale Model. Simul., 6 (2007), pp. 319–346, https://doi.org/ 10.1137/060662587.
- [6] M. Arshad, E.-J. Park, and D.-w. Shin, Analysis of multiscale mortar mixed approximation of nonlinear elliptic equations, Comput. Math. Appl., 75 (2018), pp. 401–418, https://doi. org/10.1016/j.camwa.2017.09.031.
- [7] G. R. BARRENECHEA, F. JAILLET, D. PAREDES, AND F. VALENTIN, The multiscale hybrid mixed method in general polygonal meshes, Numer. Math., 145 (2020), pp. 197–237.
- [8] F. Ben Belgacem, The mixed mortar finite element method for the incompressible Stokes problem: convergence analysis, SIAM J. Numer. Anal., 37 (2000), pp. 1085–1100, https://doi.org/10.1137/S0036142997329220.
- [9] D. BOFFI, F. BREZZI, AND M. FORTIN, Mixed Finite Element Methods and Applications, Springer Ser. Comput. Math. 44, Springer, New York, 2013.
- [10] W. M. BOON, A parameter-robust iterative method for Stokes-Darcy problems retaining local mass conservation, ESAIM Math. Model. Numer. Anal., 54 (2020), pp. 2045–2067, https://doi.org/10.1051/m2an/2020035.
- [11] W. M. BOON, J. M. NORDBOTTEN, AND I. YOTOV, Robust discretization of flow in fractured porous media, SIAM J. Numer. Anal., 56 (2018), pp. 2203–2233, https://doi.org/10.1137/ 17M1139102.

- [12] S. C. Brenner, Korn's inequalities for piecewise H1 vector fields, Math. Comp., 73 (2004), pp. 1067–1087.
- [13] M. DISCACCIATI, E. MIGLIO, AND A. QUARTERONI, Mathematical and numerical models for coupling surface and groundwater flows, Appl. Numer. Math., 43 (2002), pp. 57–74.
- [14] O. Duran, P. R. Devloo, S. M. Gomes, and F. Valentin, A multiscale hybrid method for darcy's problems using mixed finite element local solvers, Comput. Methods Appl. Mech. Engrg., 354 (2019), pp. 213–244.
- [15] B. Flemisch, M. Darcis, K. Erbertseder, B. Faigle, A. Lauser, K. Mosthaf, S. Müthing, P. Nuske, A. Tatomir, M. Wolff, and R. Helmig, DuMu<sup>x</sup>: DUNE for multi- {phase, component, scale, physics, ...} flow and transport in porous media, Advances Water Resources, 34 (2011), pp. 1102–1112, https://doi.org/10.1016/j.advwatres.2011.03.007.
- [16] G. P. GALDI, An Introduction to the Mathematical Theory of the Navier-Stokes Equations: Linearized Steady Problems, Vol. I, Springer, New York, 1994.
- [17] J. GALVIS AND M. SARKIS, Non-matching mortar discretization analysis for the coupling Stokes-Darcy equations, Electron. Trans. Numer. Anal., 26 (2007), pp. 350–384.
- [18] B. Ganis and I. Yotov, Implementation of a mortar mixed finite element method using a multiscale flux basis, Comput. Methods Appl. Mech. Engrg., 198 (2009), pp. 3989–3998, https://doi.org/10.1016/j.cma.2009.09.009.
- [19] V. GIRAULT, D. VASSILEV, AND I. YOTOV, Mortar multiscale finite element methods for Stokes-Darcy flows, Numer. Math., 127 (2014), pp. 93–165, https://doi.org/10.1007/ s00211-013-0583-z.
- [20] R. GLOWINSKI AND M. F. WHEELER, Domain decomposition and mixed finite element methods for elliptic problems, in First International Symposium on Domain Decomposition Methods for Partial Differential Equations, R. Glowinski, G. H. Golub, G. A. Meurant, and J. Periaux, eds., SIAM, Philadelphia, 1988, pp. 144–172.
- [21] C. HARDER, D. PAREDES, AND F. VALENTIN, A family of multiscale hybrid-mixed finite element methods for the Darcy equation with rough coefficients, J. Comput. Phys., 245 (2013), pp. 107–130, https://doi.org/10.1016/j.jcp.2013.03.019.
- [22] C. HARDER AND F. VALENTIN, Foundations of the MHM method, in Building Bridges: Connections and Challenges in Modern Approaches to Numerical Partial Differential Equations, Springer, New York, 2016, pp. 401–433.
- [23] E. KHATTATOV AND I. YOTOV, Domain decomposition and multiscale mortar mixed finite element methods for linear elasticity with weak stress symmetry, ESAIM Math. Model. Numer. Anal., 53 (2019), pp. 2081–2108, https://doi.org/10.1051/m2an/2019057.
- [24] H. H. KIM AND C.-O. LEE, A Neumann-Dirichlet preconditioner for a FETI-DP formulation of the two-dimensional Stokes problem with mortar methods, SIAM J. Sci. Comput., 28 (2006), pp. 1133–1152, https://doi.org/10.1137/030601119.
- [25] T. Koch, D. Gläser, K. Weishaupt, S. Ackermann, M. Beck, B. Becker, S. Burbulla, H. Class, E. Coltman, S. Emmert, T. Fetzer, C. Grüninger, K. Heck, J. Hommel, T. Kurz, M. Lipp, F. Mohammadi, S. Scherrer, M. Schneider, G. Seitz, L. Stadler, M. Utz, F. Weinhardt, and B. Flemisch, DuMu<sup>x</sup> 3—an open-source simulator for solving flow and transport problems in porous media with a focus on model coupling, Comput. Math. Appl., 81 (2021), pp. 423–443, https://doi.org/10.1016/j.camwa.2020.02.012.
- [26] W. J. LAYTON, F. SCHIEWECK, AND I. YOTOV, Coupling fluid flow with porous media flow, SIAM J. Numer. Anal., 40 (2002), pp. 2195–2218 (2003), https://doi.org/10.1137/ S0036142901392766.
- [27] J. LI AND O. WIDLUND, BDDC algorithms for incompressible Stokes equations, SIAM J. Numer. Anal., 44 (2006), pp. 2432–2455, https://doi.org/10.1137/050628556.
- [28] J. M. NORDBOTTEN, W. M. BOON, A. FUMAGALLI, AND E. KEILEGAVLEN, Unified approach to discretization of flow in fractured porous media, Comput. Geosci., 23 (2019), pp. 225–237.
- [29] L. F. PAVARINO AND O. B. WIDLUND, Balancing Neumann-Neumann methods for incompressible Stokes equations, Comm. Pure Appl. Math., 55 (2002), pp. 302–335, https://doi.org/10.1002/cpa.10020.
- [30] G. PENCHEVA AND I. YOTOV, Balancing domain decomposition for mortar mixed finite element methods, Numer. Linear Algebra Appl., 10 (2003), pp. 159–180, https://doi.org/10.1002/ nla.316.
- [31] M. Peszyńska, M. F. Wheeler, and I. Yotov, Mortar upscaling for multiphase flow in porous media, Comput. Geosci., 6 (2002), pp. 73–100, https://doi.org/10.1023/A:1016529113809.
- [32] A. QUARTERONI AND A. VALLI, Domain Decomposition Methods for Partial Differential Equations, Oxford University Press, New York, 1999.
- [33] A. QUARTERONI AND A. VALLI, Numerical Approximation of Partial Differential Equations, Springer Ser. Comput. Math. 23, Springer, New York, 2008.

- [34] L. R. SCOTT AND S. ZHANG, Finite element interpolation of nonsmooth functions satisfying boundary conditions, Math. Comp., 54 (1990), pp. 483–493, https://doi.org/10.2307/ 2008497.
- [35] R. Stenberg, Analysis of mixed finite elements methods for the Stokes problem: A unified approach, Math. Comp., 42 (1984), pp. 9–23, https://doi.org/10.2307/2007557.
- [36] A. TOSELLI AND O. WIDLUND, Domain Decomposition Methods—Algorithms and Theory, Springer Ser. Comput. Math. 34, Springer, New York, 2005.
- [37] D. VASSILEV, C. WANG, AND I. YOTOV, Domain decomposition for coupled Stokes and Darcy flows, Comput. Methods Appl. Mech. Engrg., 268 (2014), pp. 264–283, https://doi.org/10. 1016/j.cma.2013.09.009.